Electronic Supplementary Material (ESI) for Inorganic Chemistry Frontiers.

Pd(II)-based Polyoxometalate Polymers as Highly Efficient Heterogeneous Catalysts for Suzuki-Miyaura Reactions

Jiayou Hou, Lin Zhang, Yunjing Li, Yan Xia, Hai Fu, Peipei Guo*, Yuhui Ao*

School of Chemistry and Life Science, Advanced Institute of Materials Science, Changchun University of Technology, Changchun, Jilin, P. R. China.

Email: Mr.fuhai@163.com.

Table of Contents

1 Experimental section

Materials and general methods:

The inorganic and organic reagents and solvents were all purchased on Sigma-Aldrich and used without any additional purification. The Single-crystal X-ray crystallography was collected on a BRUKER D8 Venture Single-crystal Diffractometer. The Powder X-ray Diffraction (PXRD) was carried out on a Rigaku Smartlab X-ray Diffractometer. The ^{1}H NMR and ^{13}C NMR spectra were obtained in DMSO-d_6 and $CDCl_3$-d on a BRUKER AVANCE HD 400 MHz spectrometer. The thermal stability of the compounds was measured on TA TGAQ500. The Pd and Mo elements were analyzed on a Perkin Elmer Optima 8000 (ICP) Optical Emission Spectrometer. The Fourier-Transform Infrared Spectra (FT-IR) was obtained in Nicolet iS 50. The Field-Emission Scanning Electron Microscope (FE-SEM) and Oxford EDS (EDX) images were obtained using a JEOL JSM-7610F; Oxford EDS. The X-ray photoelectron spectroscopy (XPS) was obtained on Thermo ESCALAB 250Xi. Transmission electron microscopy (TEM) images were obtained on Thermo FEI F200X and Super-X (EDS).

Synthesis of 1 $[Pd(II)(H_2O)_4]_{0.5}[Mo_7O_{24}]\cdot 5H_3O\cdot 3H_2O$

A mixture of $Pd(OAC)_2$ (20 mg, 0.089 mmol), $(NH_4)_6Mo_7O_{24}\cdot 4H_2O$ (200 mg, 0.340 mmol), H_2O/CH_3CN = 4/1 (H_2O = 8.0 ml, CH_3CN = 2.0 ml) was vigorously stirred for about 30 minutes at room temperature. After that, the final pH value was adjusted to 3.6-4.5 with 1M HCl aq sealed in a glass autoclave reactor (15 mL), kept under 120 °C for 48 hours. After cooling to room temperature at the rate of 10 °C per hour, it stood at 4 °C for another 48 hours. Colorless transparent block-shaped crystals of **1** were received, washed with ethanol and dried in vacuum for 8 hours at room temperature. Transparent crystals of **1** were collected in 62% yields based on Mo. Calcd: Pd 4.11 wt%, 0.75 mol%, Mo 51.92 wt%, 10.63 mol%, The Pd and Mo elements were analyzed on a Perkin Elmer Optima 8000 (ICP) Optical Emission Spectrometer. Found: Pd 4.03 wt%, 0.74 mol%, Mo 51.80 wt%, 10.52 mol%.

Synthesis of 2 and 2' $[Pd(II)(H_2O)_4]_2[Mo_7O_{24}]\cdot 2H_3O\cdot H_2O$

A mixture of $Pd(OAC)_2$ (20 mg, 0.089 mmol), **1** (100 mg, 0.077 mmol), H_2O/CH_3CN = 1/1 (H_2O = 5.0ml, CH_3CN = 5.0ml) was vigorously stirred for about 30 minutes at room temperature. After that, the final pH value of the mixture was adjusted nearly to 5.0-6.2 with 1M HCl aq sealed in a glass autoclave reactor (15 mL), kept under 130 °C for 72 hours. After cooling to room temperature at the rate of 10 °C per hour, it stood at room temperature for another 48 hours. Colorless transparent lamellar crystals of **2** were obtained, washed with ethanol, and dried in the air. **2'** were prepared under the similar mixed solvothermal procedures with **2**. Transparent crystals of **2** and **2'** were collected in 64%, 60% yields based on Mo, respectively. Calcd: Pd 14.50 wt%, 2.94 mol%, Mo 45.74 wt%, 10.29 mol%, The Pd and Mo elements were analyzed on a Perkin Elmer Optima 8000 (ICP) Optical Emission Spectrometer. Found: Pd 14.83 wt% and 14.45 wt%, 2.90 mol%,2.92 mol%, Mo 45.72 wt% and 45.30 wt%, 10.40 mol%, 10.18 mol%.

Synthesis of 3 $[Pd(II)(H_2O)_4][Mo_4O_{13.5}]\cdot H_3O$

A mixture of $Pd(OAC)_2$ (10 mg, 0.044 mmol), **2** (110 mg, 0.075 mmol), H_2O/CH_3CN = 2/8, (H_2O = 2.0 ml, CH_3CN = 8.0 ml) was stirred for 10 minutes at room temperature. After that, the final pH value was adjusted to 3.6-4.2 with 1M HCl aq sealed in a glass autoclave reactor (15 mL), kept under 140 °C for 96 hours. After cooling to room temperature at the rate of 10°C per hour, colorless transparent block-shaped crystals of **3** were obtained, Washed three times with 20 ml water, and dried in the air. Transparent crystals of **3** were collected in 58% yields based on Mo. Calcd: Pd 13.35 wt%, 2.90 mol%, Mo 48.15 wt%, 11.60 mol%. The Pd and Mo elements were analyzed on a Perkin Elmer Optima 8000 (ICP) Optical Emission Spectrometer. Found: Pd 13.45 wt %, 2.80 mol%, 48.40 wt%, 11.40 mol%.

Synthesis of 4 $[Pd(II)(H_2O)_4][Pd(II)(H_2O)_3Mo_4O_{14}]\cdot 2H_2O$

A mixture of $Pd(OAC)_2$ (20 mg, 0.089 mmol), **2** (80 mg, 0.054 mmol), H_2O/CH_3CN = 2/8 (H_2O = 2.0 ml, CH_3CN=8.0 ml) was stirred for about 15 minutes at room temperature. After that, the final pH value was adjusted to 2.3-2.8 with 1M HCl aq sealed in a glass autoclave reactor (15 mL), kept under 160°C for 96 hours. After cooling to room temperature at the rate of 10°C per hour, it stood 4 °C for another 120 hours. Then gained colorless transparent block-shaped crystals of **4** were obtained, Washed three times with 10 ml ethanol, and dried in vacuum for 3 hours at room temperature. Transparent crystals of **4** were collected in 50% yields based on Mo. Calcd: Pd 21.67 wt%, 4.26 mol%, Mo 39.06 wt%, 8.52 mol%. The Pd and Mo elements were analyzed on a Perkin Elmer Optima 8000 (ICP) Optical Emission Spectrometer. Found: Pd 21.58 wt%, 4.13 mol%, Mo 38.86 wt%, 8.32 mol%.

Suzuki–Miyaura cross-coupling reactions

C_2H_5OH (10.0 mL), arylboronic acid or its derivatives (0.75 mmol), aryl halides or its derivatives (0.5 mmol), K_2CO_3 (207.3 mg, 1.5 mmol,), catalyst **4** (15.00 mg, 0.015mmol), were added together with a magnetic stirring bar in a 20ml glass round bottom flask. The mixture was stirred in a glass round bottom flask at the given optimal reaction temperature under the conventional condition. After the reactions, the organic phase was separated though filter, then solid catalysts were recycled and reused. Evaporate organic phase, and then the crudes were extracted three times with CH_2Cl_2 (5.0 mL) and H_2O (5.0 mL). The crudes were purified by silica gel column chromatography (Eluent: Petroleum ether and ethyl acetate in the range of 1:1 to 10:1), and calculated the separation yield. (Yield=actual output/theoretical output*100%). The ^1H NMR and ^{13}C NMR spectra were obtained in DMSO-d_6 and $CDCl_3$-d on a BRUKER AVANCE HD 400 MHz spectrometer to verify the product yield.

Single-crystal X-ray crystallography

A diffractive quality single crystal was mounted on a glass fiber, and the crystallographic data were collected at 298 (K) for **1**, **2**, **2'**, **3** and 200 (K) for **4** on a Bruker D8 Venture diffractometer using graphite monochromatic Mo-Kα radiation (λ = 0.71073 Å) and Smart APEX II

diffractometer. The crystal data of **1**, **2**, **2'**, **3** and **4** were solved by direct method and refined by full-matrix least-squares method on F^2 using the crystallographic software package Shelxtl-2018 and Olex 2.[1-4] Not all the non-hydrogen atoms were refined with anisotropic thermal parameters. The H atoms on the C atoms were fixed in the calculated positions. The details of the refinements are all in table S1 in the supporting information. The details of the refinement process are attached in the CIF files; CCDC 2042532, 2042534, 2042535, 2042536, 2042537 for **1-4** containing the crystal-lographic data. The CIF files can be obtained free of charge, by contacting CCDC, 12 Union Road, Cambridge CB21EZ, UK via fax (+44 1223 336033) or by e-mail (data_request@ ccdc.cam.ac.uk).

(1) G.M. Sheldrick. SHELXS/L-97, Programs for Crystal Structure Refinement, University of Göttingen, Germany **(1997)**.
(2) G.M. Sheldrick. SHELX-2017, Programs for Crystal Structure Determination, University of Göttingen, Germany **(2017)**.
(3) Bruker. Xscans. Bruker AXS Inc., Madison, Wisconsin **(1998)**.
(4) O.V. Dolomanov, L.J. Bourhis, R.J. Gildea, J.A.K. Howard, H. Puschmann, OLEX 2: A complete structure solution, refinement and analysis program., *J. Appl. Cryst* 2009, **42***,* 339-341.

2 Crystal data compounds of 1-4

Table S1. Crystal data and structure refinements.

Compounds	**1**	**2**	**2'**	**3**	**4**
Empirical formula	$[Pd(H_2O)_4]_{0.5}[Mo_7O_{24}]\cdot 5H_3O\cdot 3H_2O$	$[Pd(H_2O)_4]_2[Mo_7O_{24}]\cdot 2H_3O\cdot H_2O$	$[Pd(H_2O)_4]_2[Mo_7O_{24}]\cdot 2H_3O\cdot H_2O$	$[Pd(H_2O)_4][Mo_4O_{13.5}]\cdot H_3O$	$[Pd(H_2O)_4][Pd(H_2O)_3Mo_4O_{14}]\cdot 2H_2O$
Formula weight	1293.85	1468.50	1468.50	797.21	982.64
T/K	293	293	193	293	293
Wavelength/Å	0.71073	0.71073	0.71073	0.71073	0.71073
Cryst. syst.	Orthorhombic	Monoclinic	Monoclinic	Monoclinic	Triclinic
Space group	*Fdd*2	*C*2/*c*	*C*2/*c*	*C*2/*c*	*P*-1
a/Å	19.203(2)	29.345(5)	31.524(6)	15.445(3)	10.0495(10)
b/Å	72.352(8)	10.1725(17)	10.224(2)	20.196(4)	10.1019(10)
c/Å	8.3479(9)	19.980(3)	19.965(4)	10.591(2)	10.4574(10)
α/°	90	90	90	90	69.406(2)
β/°	90	96.914(5)	108.653(5)	91.985(2)	84.106(2)
γ/°	90	90	90	90	88.251(1)
V/ Å^3	11598(2)	5920.8(17)	6097(2)	3301.5(11)	988.51(17)
Z	16	8	8	8	2
Dcalc (mg m^{-3})	2.948	3.2767	3.1953	3.2037	3.2811
μ /mm^{-1}	3.351	4.171	4.051	4.111	4.345
F(000)	9517	5347	5395	2915	895
θ range (°)	2.68 to	2.99 to	2.73 to 25.00	8.95 to	2.957 to 28.323

	25.00	28.36		28.37	
R_{int}	0.0756	0.1979	0.0845	0.0483	0.0461
Data/restraints/ parameters	5103/0/397	5214/0/350	5348/0/332	3975/0/224	4916/0/247
GOF on F^2	1.058	1.1157	1.0234	1.0630	1.0232
$R_1{}^a/wR_2{}^b$ [$I > 2\sigma(I)$]	0.0337/0.0858	0.0475/0.0885	0.0750/ 0.1655	0.0231/0.0589	0.0341/0.1016
$R_1{}^a/wR_2{}^b$ (all data)	0.0355/0.0871	0.0641/0.0947	0.0801/ 0.1682	0.0259/0.0614	0.0370/0.1111

$^aR_1 = \Sigma||F_o|-|F_c||\Sigma/|F_o|$; $^b wR_2 = \Sigma[w(F_o^2 - F_c^2)^2]/ \Sigma[w(F_o^2)^2]^{1/2}$.

3 Supplementary structural figures and H-bonding of 1-4

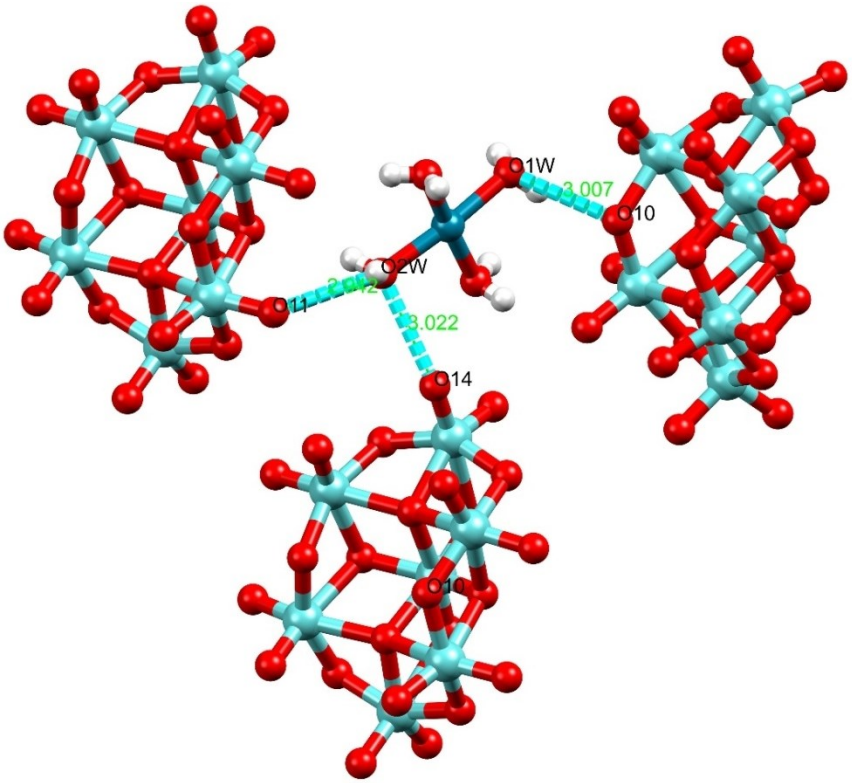

Fig. S1 H-bonds and the ball and stick representation of **1**. Mo atoms blue balls, O atoms red balls, Pd atoms dark blue balls, H atoms light grey balls, H-bonds dash blue sticks.

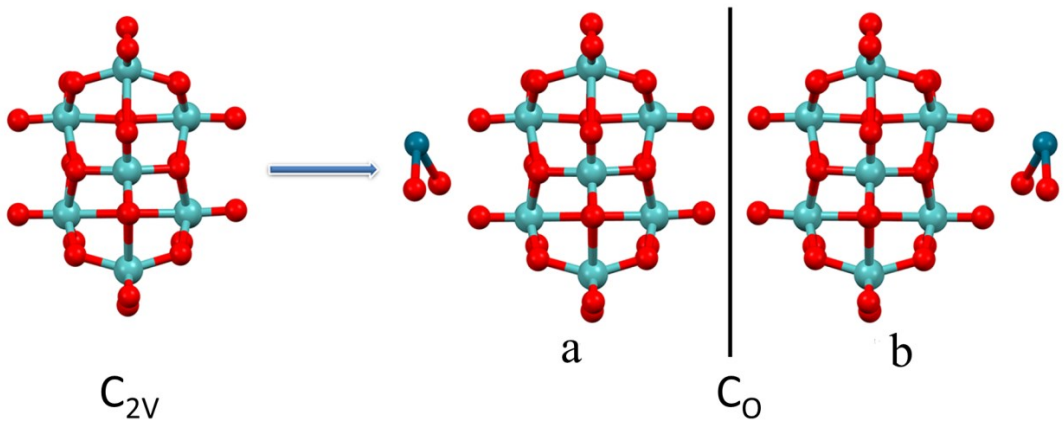

Fig. S2 Two kinds of chiral POMs secondary building units SBUs, the symmetry evolvement of structure induced by metal center Pd(II), (a) the S configuration, (b) the R configuration. Mo atoms blue balls, O atoms red balls, Pd atoms dark blue balls.

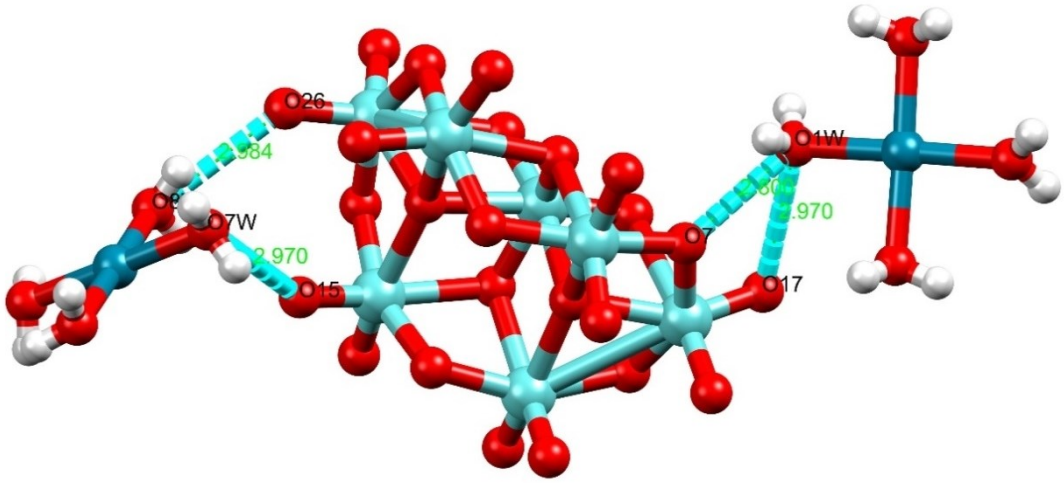

Fig. S3 H-bonds and the ball and stick representation of **2**. Mo atoms blue balls, O atoms red balls, Pd atoms dark blue balls, H atoms light grey balls, H-bonds dash blue sticks.

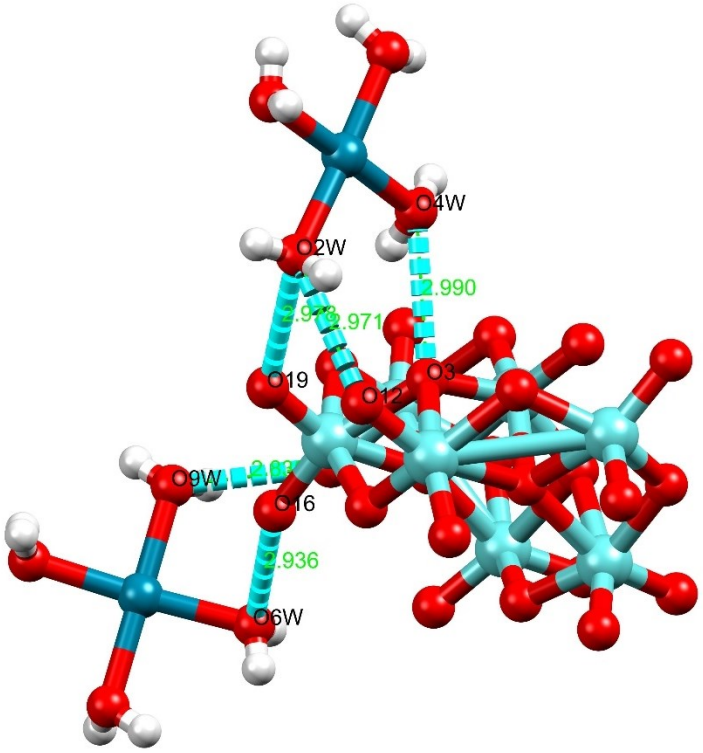

Fig. S4 H-bonds and the ball and stick representation of **2'**. Mo atoms blue balls, O atoms red balls, Pd atoms dark blue balls, H atoms light grey balls, H-bonds dash blue sticks. $[Pd(H_2O)_4]_2[Mo_7O_{24}]\cdot 2H_3O\cdot H_2O$.

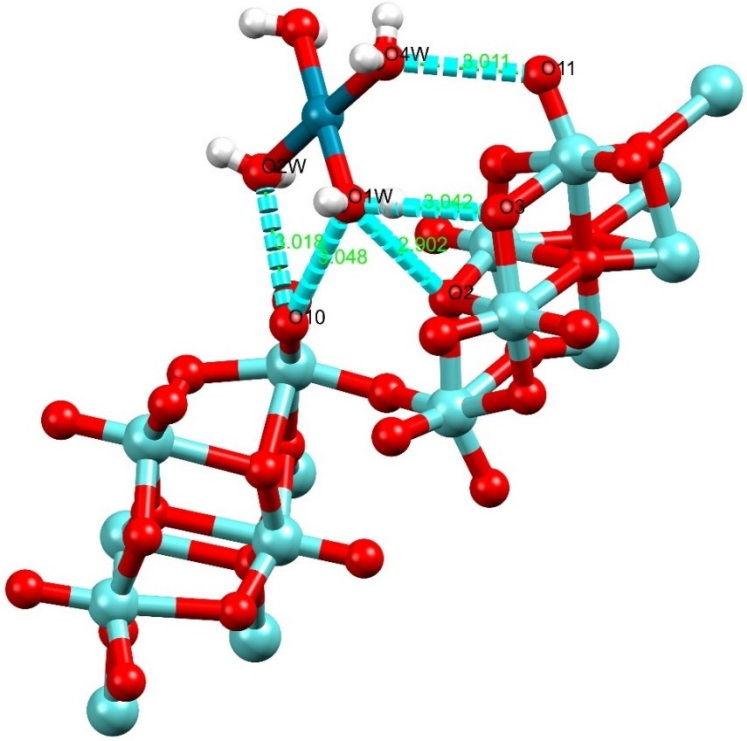

Fig. S5 H-bonds and the ball and stick representation of **3**. Mo atoms blue balls, O atoms red balls,

Pd atoms dark blue balls, H atoms light grey balls, H-bonds dash blue sticks.

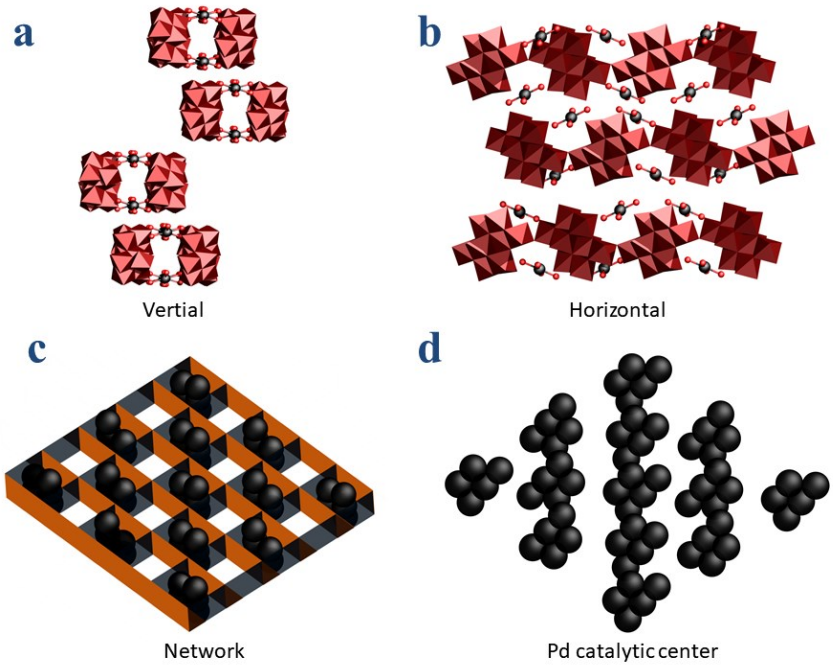

Fig. S6 (a) $Pd(II)(H_2O)_4$ and $^1/_\infty[Mo_8O_{27}]^{6-}$ chain vertical view of **3**, Mo atoms black balls, O atoms red balls, MoO_6 red octahedra; (b) $Pd(II)(H_2O_4)$ and $^1/_\infty[Mo_8O_{27}]^{6-}$ chain Horizontal view of **3**, Pd atoms black balls, O atoms red balls, MoO_6 red octahedra; (c) Pd is scattered in a two-dimensional network, The dark yellow strip is a simplification of the $^1/_\infty[Mo_8O_{27}]^{6-}$ chain, The black band is a virtual way of segmentation. (d) The ball representation of evenly dispersed bare palladium activity centers.

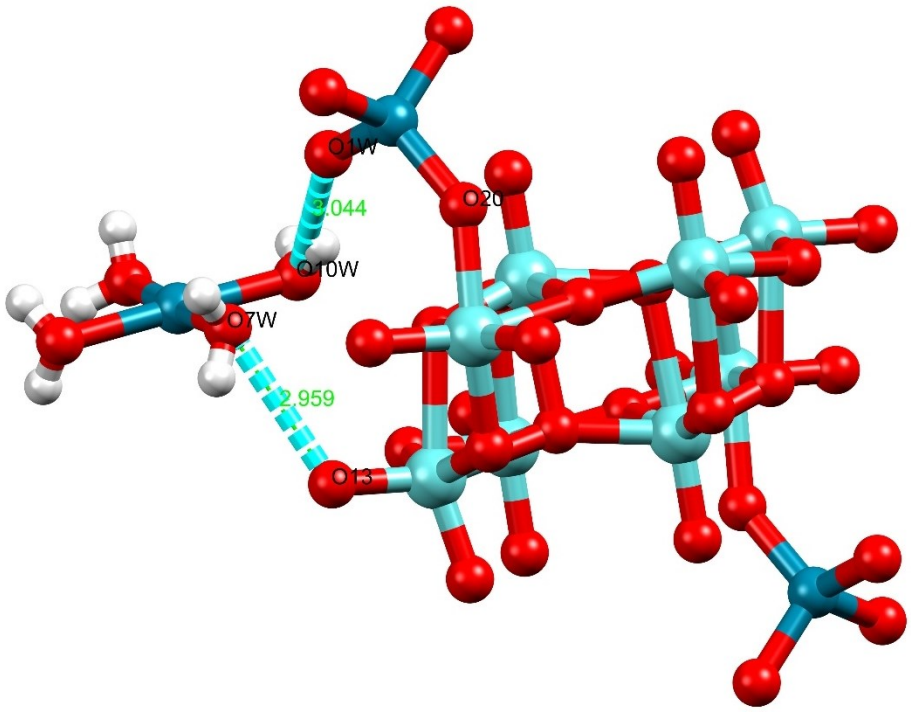

Fig. S7 H-bonds and ball and stick representation of **4**, the POMs and Pd are connected by covalent bond Pd-O-Mo. Mo atoms light blue balls, O atoms red balls, Pd atoms dark blue balls, H atoms light grey balls, H-bonds dash blue sticks. Pd-O bond, the covalent bonds between Mo and Pd two-colour sticks (Pd1-O7w 2.04099(14)Å, Pd1-O8w 2.06146(14)Å, Pd1-O9w 2.04124(14)Å, Pd1-O10w 2.03665(13)Å, Pd3-O20 1.85043(18)Å, Pd3-O1w 1.73897(14)Å, Pd3-O2w 1.74474(14) Å, Pd3-O3w 1.73666(14) Å).

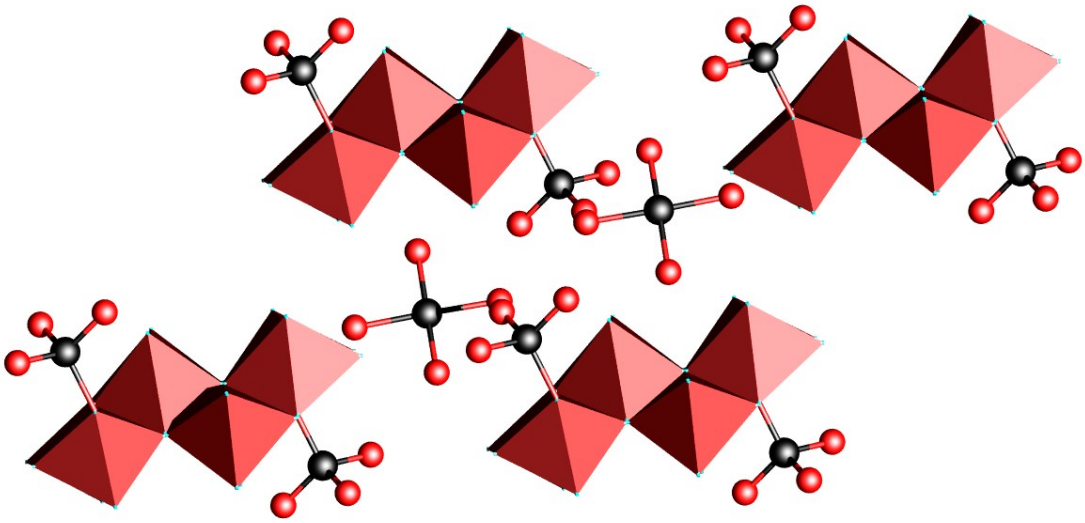

Fig. S8 Pd(II)$(H_2O)_4$ counter cations are connected with [Pd(II)$(H_2O)_3(Mo_8O_{28})]^{4-}$ anions to extend to 3D super molecules through hydrogen bonds, and the Pd centers are uniformly dispersed in the 3D super molecular network. Pd atoms black balls, O atoms red balls, MoO_6 red octahedral.

Table S2. H-bonding geometry (Å) in **1-4**

Compound **1**		Compound **2**		Compound **2'**		Compound **3**		Compound **4**	
O1W-H···O10	3.007	O1W-H···O7	2.800	O2W-H···O12	2.971	O1W-H···O2	3.042	O1W-H···O10w	3.044
O2W-H···O11	2.942	O1W-H···O17	2.970	O2W-H···O19	2.978	O1W-H···O3	2.902	O7W-H···O13	2.959
O2W-H···o14	3.022	O8W-H···O15	2.970	O4W-H···O3	2.990	O1W-H···O10	3.048		
		O8W-H···O26	2.984	O6W-H···O16	2.936	O2W-H···O10	3.018		
				O9W-H···O18	2.839	O4W-H···O11	3.011		

4 TGA of 3 and 4, FT-IR of 4, PXRD of 3, XRD patterns peaks of 4, FESEM-EDX and TEM-EDX images of 4

Thermogravimetric analysis (TGA) of **3** and **4**

10.0 mg dry crystals of **3** were weighed at the room temperature, and TGA were measured by flowing dry nitrogen with a heating and cooling rate of 20 °C min^{-1} on a TA TGAQ500 between 40 and 650 °C. The thermogravimetric analysis (TGA) of **3** (Fig. S9), reveals a weight loss of nearly 3 % from 225 °C to 310 °C, which corresponds to the crystal waters, a weight loss of about 12.0% from 310 °C to 360 °C, which corresponds to the coordinated waters from $Pd(II)(H_2O)_4$, The third mass loss begins at 360 °C, and is associated with the decomposition of $^1/_\infty[Mo_8O_{27}]^{6-}$ anions.

8.0 mg dry crystals of **4** were weighed at the room temperature, and TGA were measured by flowing dry nitrogen with a heating and cooling rate of 20 °C min^{-1} on a TA TGAQ500 between 40 and 650 °C. The thermogravimetric analysis (TGA) of **4** (Fig. S9), reveals a weight loss of about 3.2 % from 92 °C to 230 °C, which corresponds to the crystal waters, a weight loss of about 13.8% from 230 °C to 360 °C, which corresponds to the coordinated waters from $[Pd(II)(H_2O)_4][Pd(II)(H_2O)_3][Mo_4O_{14}]$, The third mass loss begins at 360 °C, and is associated with the decomposition of $[Mo_8O_{28}]^{8-}$ anions.

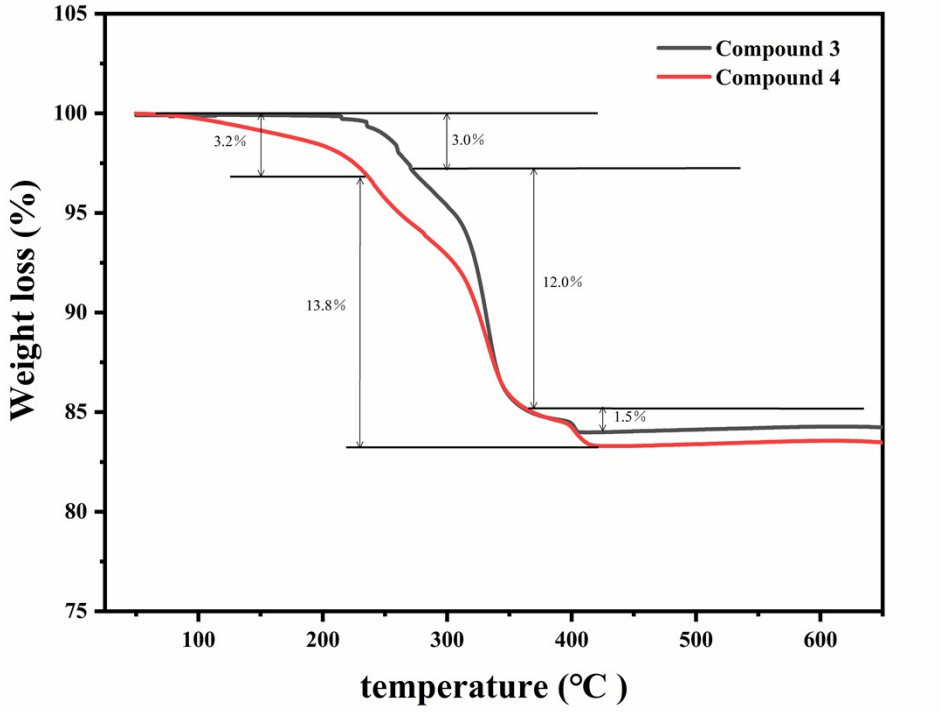

Fig. S9 Thermogravimetric analysis (TGA) of **3** and **4**

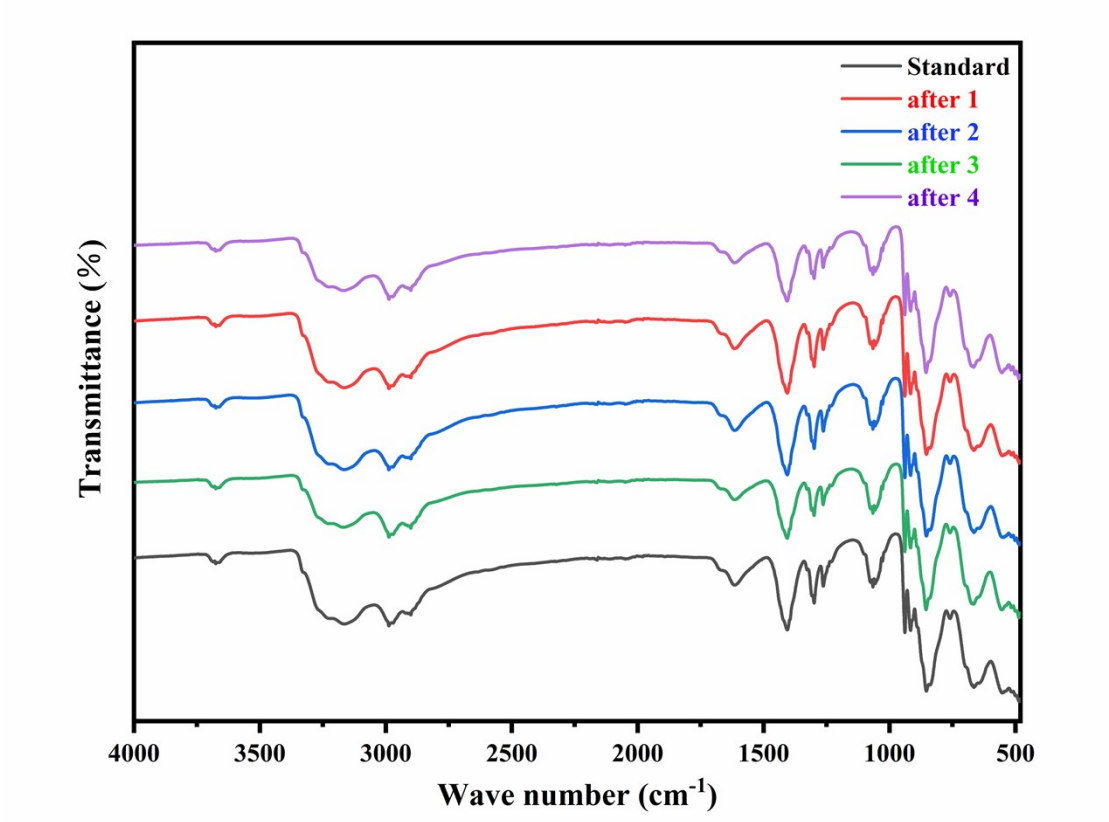

Fig. S10 Fourier-Transform Infrared Spectra (FT-IR) for 4; the simulation data and the data after 4 recycles of 4 in the continuous coupling reactions between bromobenzene and phenylboronic acid.

Reaction conditions: Catalyst 4 (8.0 mg, 0.010 mmol), bromobenzene (78.5 mg, 0.5 mmol), phenylboronic acid (91.44 mg, 0.75 mmol), 1.5 mmol of alkali, 8.0 mL of EtOH, 0.5 h. FTIR data (cm^{-1}): The IR spectra (600-4000 cm^{-1}) are virtually identical strongly suggesting a structure of 4. The IR spectra show the O-H absorption bands as well as typical frequencies for Mo-O and Pd-O bonds. The characteristic absorptions around 940 and 847 cm^{-1} are attributed to the Mo-O_t, Mo-O_b-Mo and Pd-O-Mo vibrations, respectively. These vibrations are somewhat red shifted compared to those of [γ-Mo_8O_{26}]. The bonds at around 2800-3300 cm^{-1} are attributed to the ν_{as} (H_2O) and vibrations. The bonds at around 1625 cm^{-1} and 1420 cm^{-1} are attributed to (H_2O) deformation vibrations. The bonds at around 3750 cm^{-1} and 3700 cm^{-1} are attributed to H_2O-Pd-H_2O deformation vibrations.

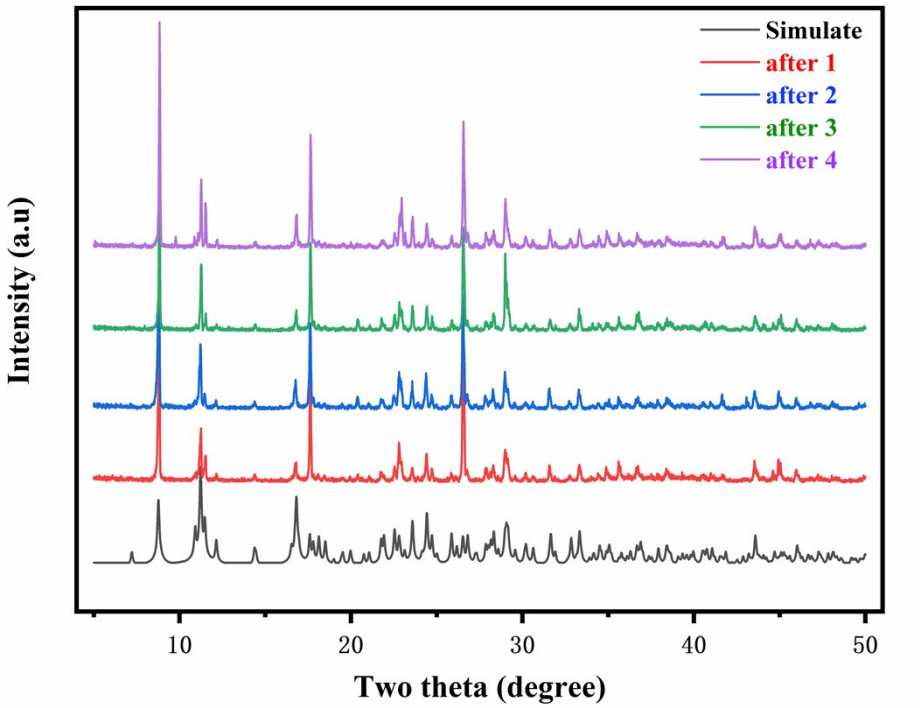

Fig. S11 Powder XRD patterns for **3**; the simulation data and the data after 4 recycles of **3** in the continuous coupling reactions between bromobenzene and phenylboronic acid. Reaction conditions: **3** (8.0 mg, 0.012 mmol), bromobenzene (78.5 mg, 0.5 mmol), phenylboronic acid (91.44 mg, 0.75 mmol), 1.5 mmol of alkali, 8.0 mL of EtOH, 0.5 h.

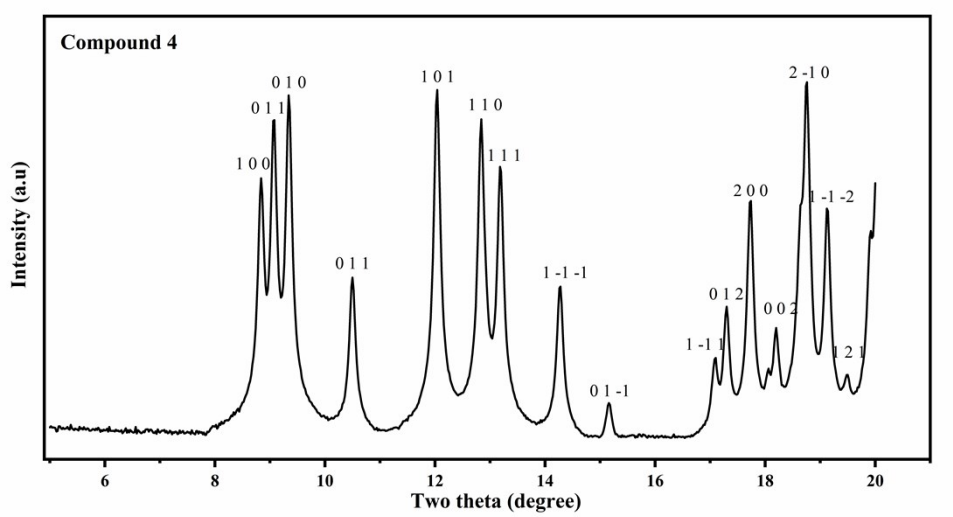

Fig. S12 The (*h k l*) in the range of 5° to 20° (2*θ*). The data is calculated by the software Hg 1.4.2 with the cif file of **4.**

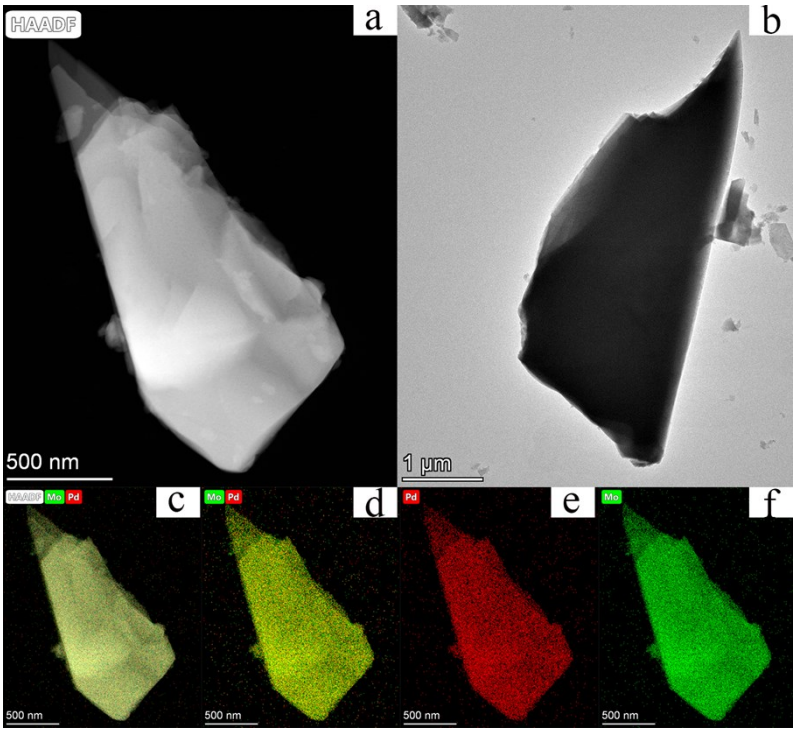

Fig. S13 (a-b) TEM images of **4,** (c-f) energy-dispersive X-ray spectroscopy (EDX)-map images of **4**.

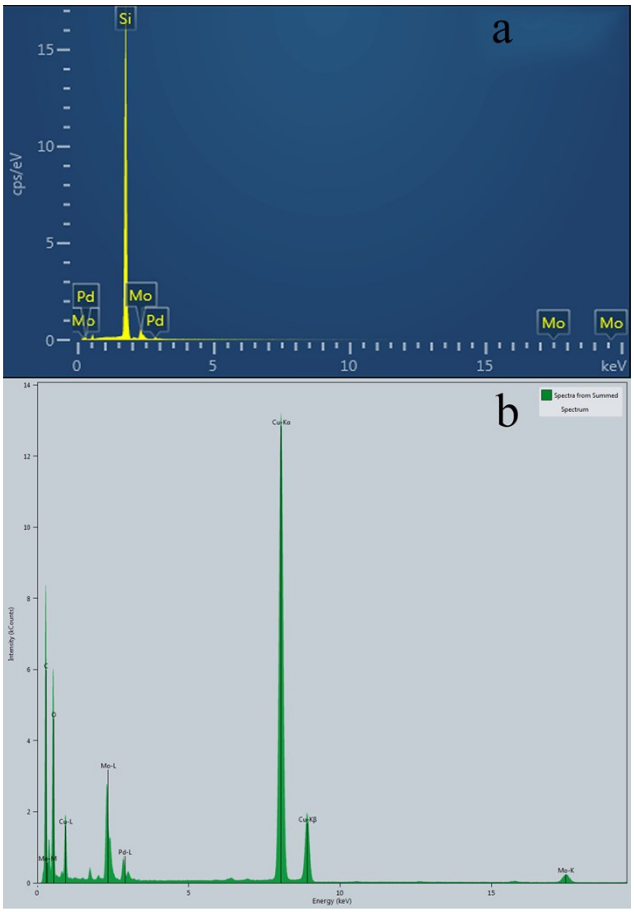

Fig. S14 (a) FESEM-EDX of **4**, (b) TEM-EDX of **4**.

5 Optimization conditions of the Suzuki coupling reaction catalyzed by 4

Table S3. Conditions of Suzuki-Miyaura coupling reactions between bromobenzene and phenylboronic acids catalyzed by **4** $[Pd(II)(H_2O)_4][Pd(II)(H_2O)_3Mo_4O_{14}]\cdot 2H_2O$ [a]

Entry	Solvent	T/℃	Time/min	Base	Yield[b] [%]
1	EtOH	45	30	K_2CO_3	99
2	EtOH	45	30	Na_2CO_3	93
3	EtOH	45	30	NaOH	86
4	EtOH	45	30	NaOAc	30
5	EtOH	45	30	KOAC	35
6	EtOH	45	30	K_3PO_4	85
7	THF	55	60	K_2CO_3	33
8	THF	55	60	K_3PO_4	61
9[c]	THF/EtOH	55	60	K_2CO_3	74
10[c]	THF/EtOH	55	60	Na_2CO_3	70

[a] Reaction conditions: Catalyst (8.0 mg, 0.010 mmol), bromobenzene (78.5 mg, 0.5 mmol), phenylboronic acid (91.44 mg, 0.75 mmol), 1.5 mmol of alkali, 8.0 mL of EtOH, 0.5 h. [b]Isolated yield, Yield= actual output/theoretical output. [c]THF/ EtOH=1/1, 4.0 ml of THF, 4.0 ml of EtOH.

6 ^{1}H NMR and ^{13}C NMR spectra

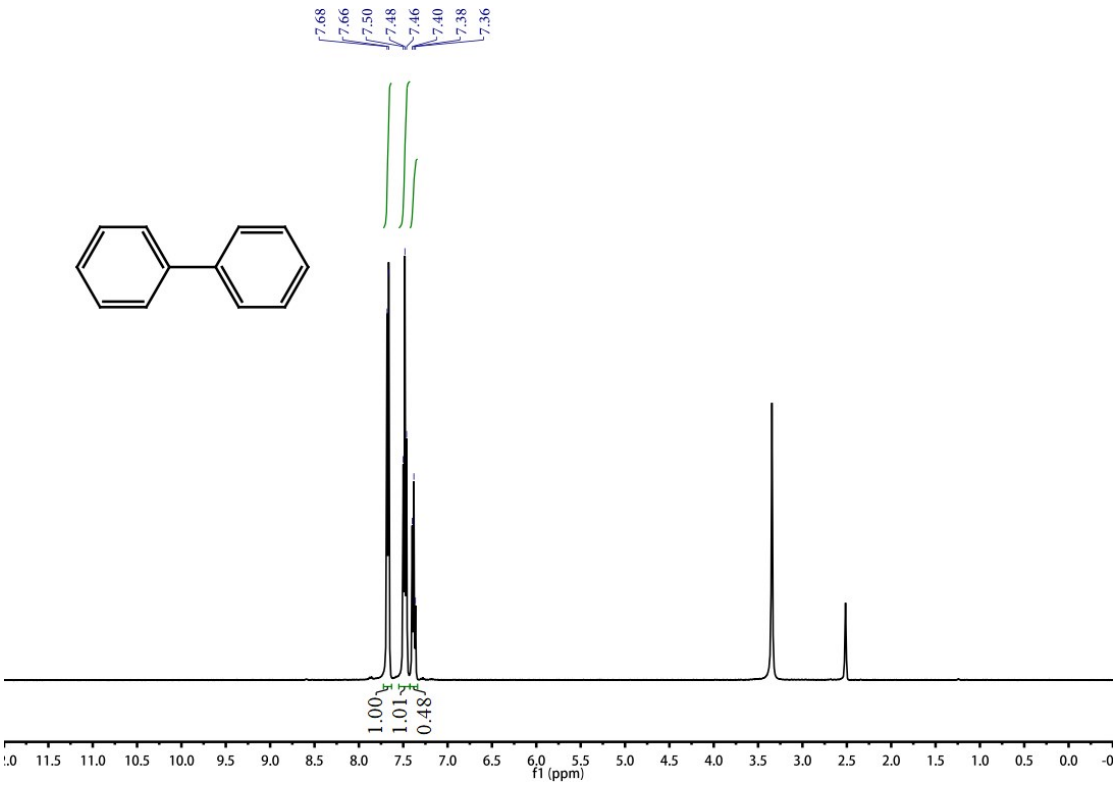

Fig. S15 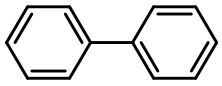 1'-biphenyl: ^{1}H NMR (400 MHz, dmso) 7.67 (d, J = 7.4 Hz, 4H), 7.48 (t, J = 7.5 Hz, 4H), 7.38 (t, J = 7.3 Hz, 2H).

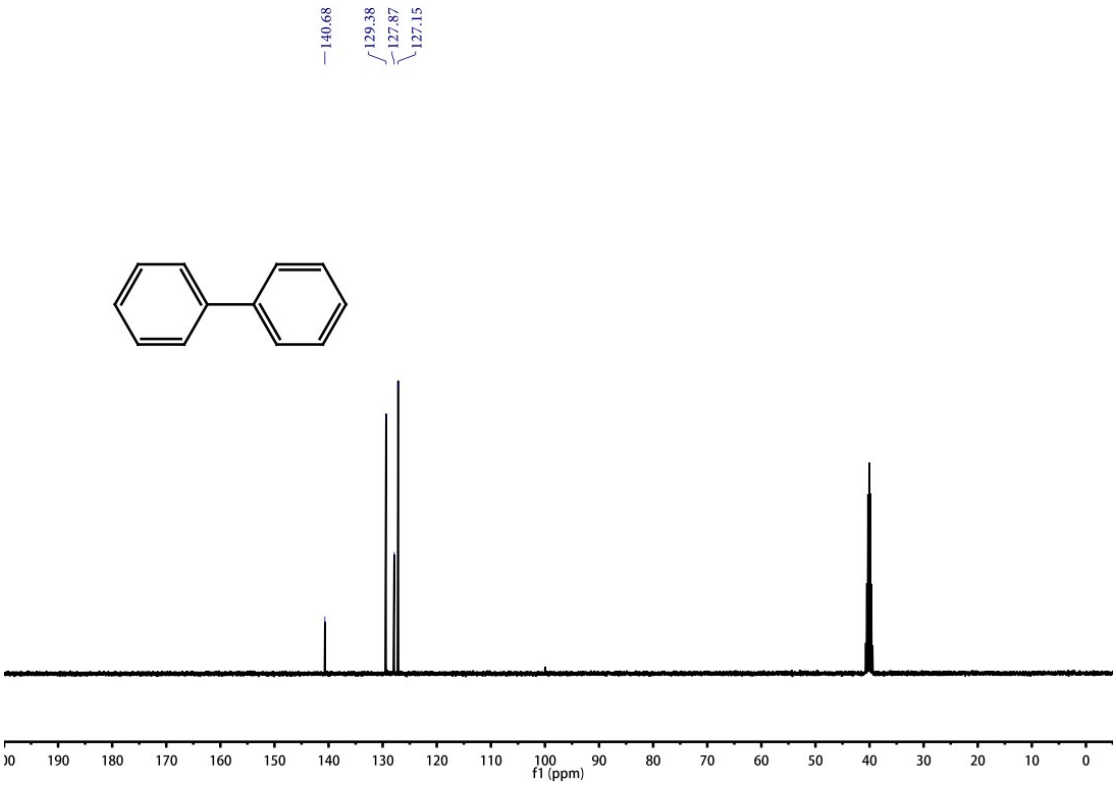

Fig. S16 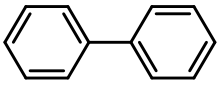 1'-biphenyl: ^{13}C NMR (100 MHz, dmso) 140.68, 129.38, 127.87, 127.15.

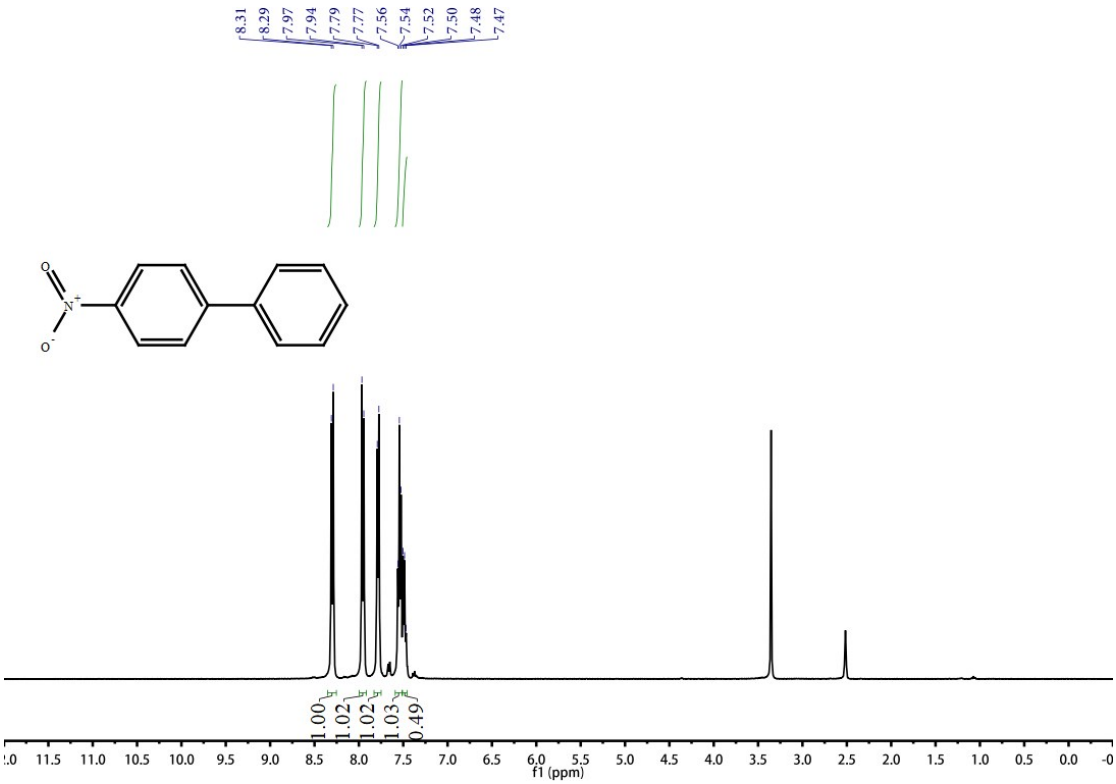

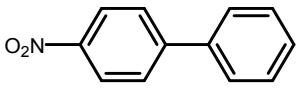

Fig. 17 4-nitro-1,1'-biphenyl: 1H NMR (400 MHz, dmso) 8.30 (d, J = 8.7 Hz，2H), 7.95 (d, J = 8.7 Hz, 2H), 7.78 (d, J = 7.4 Hz, 2H), 7.54 (t, J = 7.3 Hz , 2H), 7.51 - 7.46 (m, 3H).

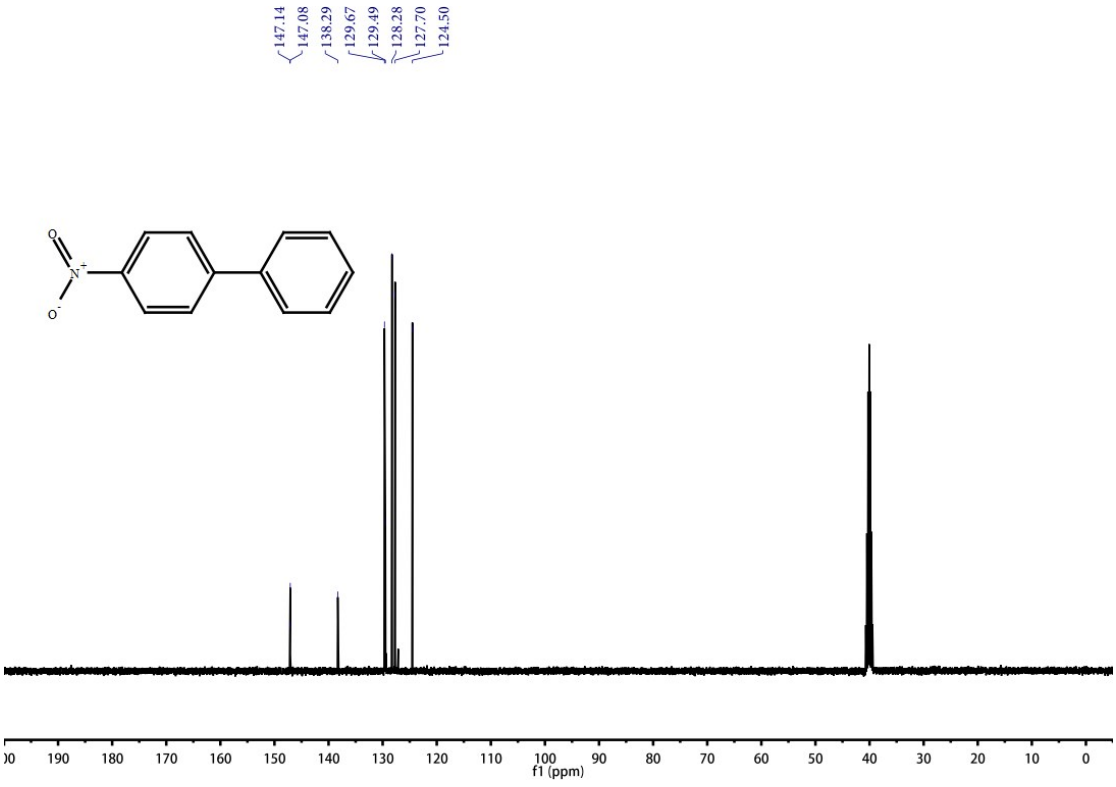

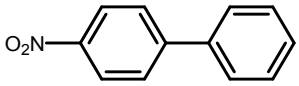

Fig. 18 4-nitro-1,1'-biphenyl:^{13}C NMR (100 MHz, dmso) 147.14, 147.08, 138.29, 129.67, 129.49, 128.28, 127.70, 124.50.

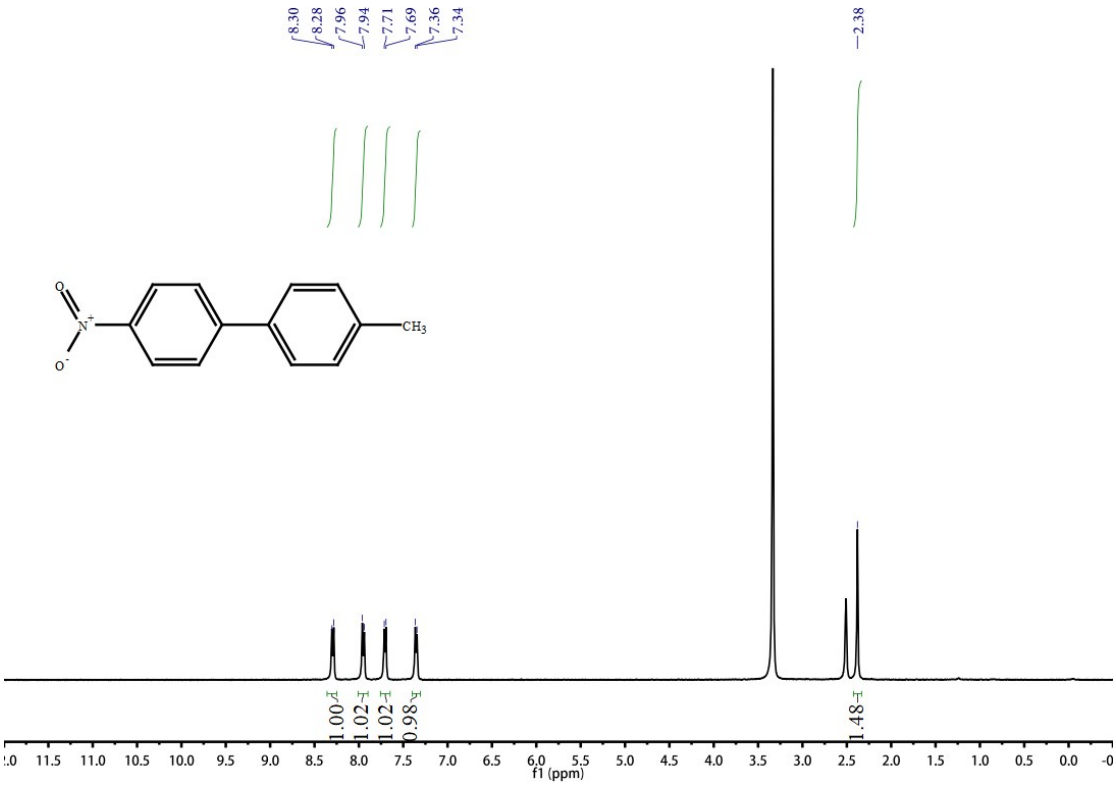

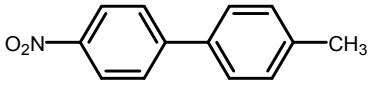

Fig. S19 4-methyl-4'-nitro-1,1'-biphenyl: ^{1}H NMR (400 MHz, dmso) 8.28 (d, *J* = 7.9 Hz, 2H) 7.95 (d, *J* = 8.7 Hz, 2H), 7.70 (d, *J* = 7.9 Hz, 2H), 7.35 (d, *J* = 7.7 Hz, 2H), 2.38 (s, 3H).

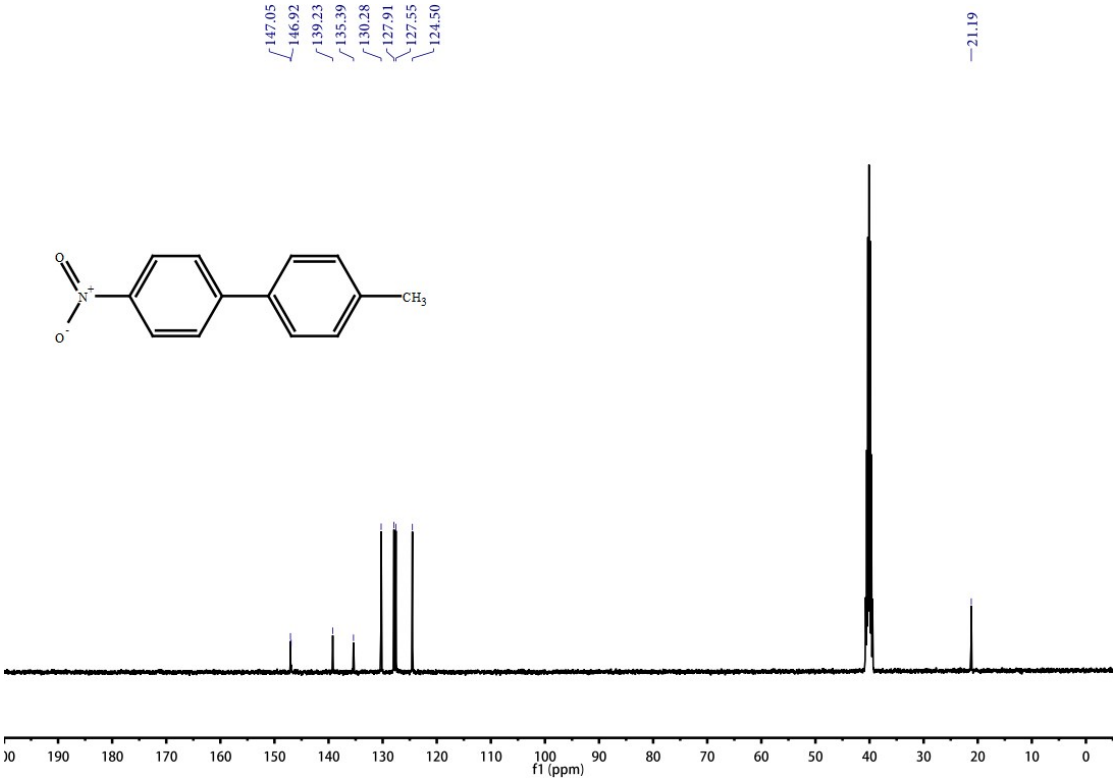

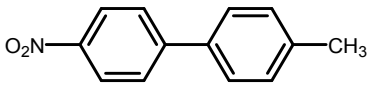

Fig. S20 4-methyl-4'-nitro-1,1'-biphenyl: ^{13}C NMR (100 MHz, dmso) 147.05, 146.92, 139.23, 135.39, 130.28, 127.91, 127.55, 124.90, 21.19.

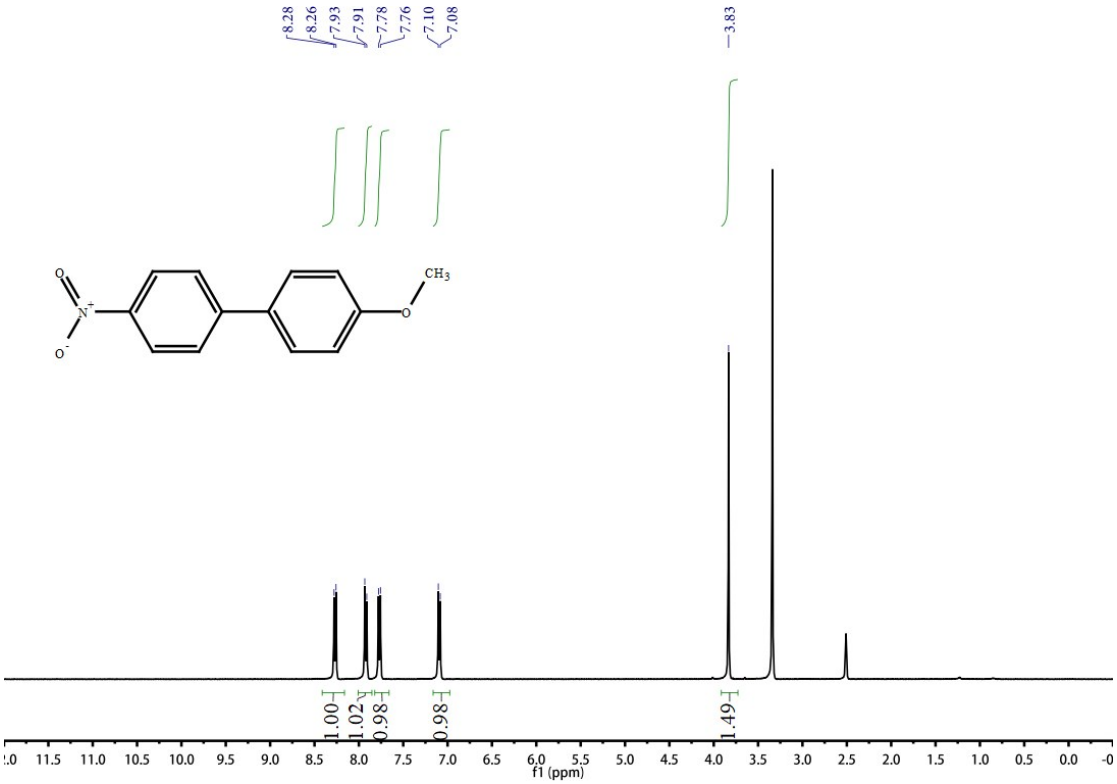

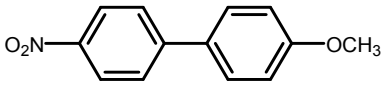

Fig. S21 4-methoxy-4'-nitro-1, 1'-biphenyl: ^{1}H NMR (400 MHz, dmso) 8.27 (d, J = 8.9 Hz, 2H), 7.92 (d, J = 9.0 Hz, 2H), 7.77 (d, J = 8.9 Hz 2H), 7.09 (d, J = 8.8 Hz, 2H), 3.83 (s, 3H).

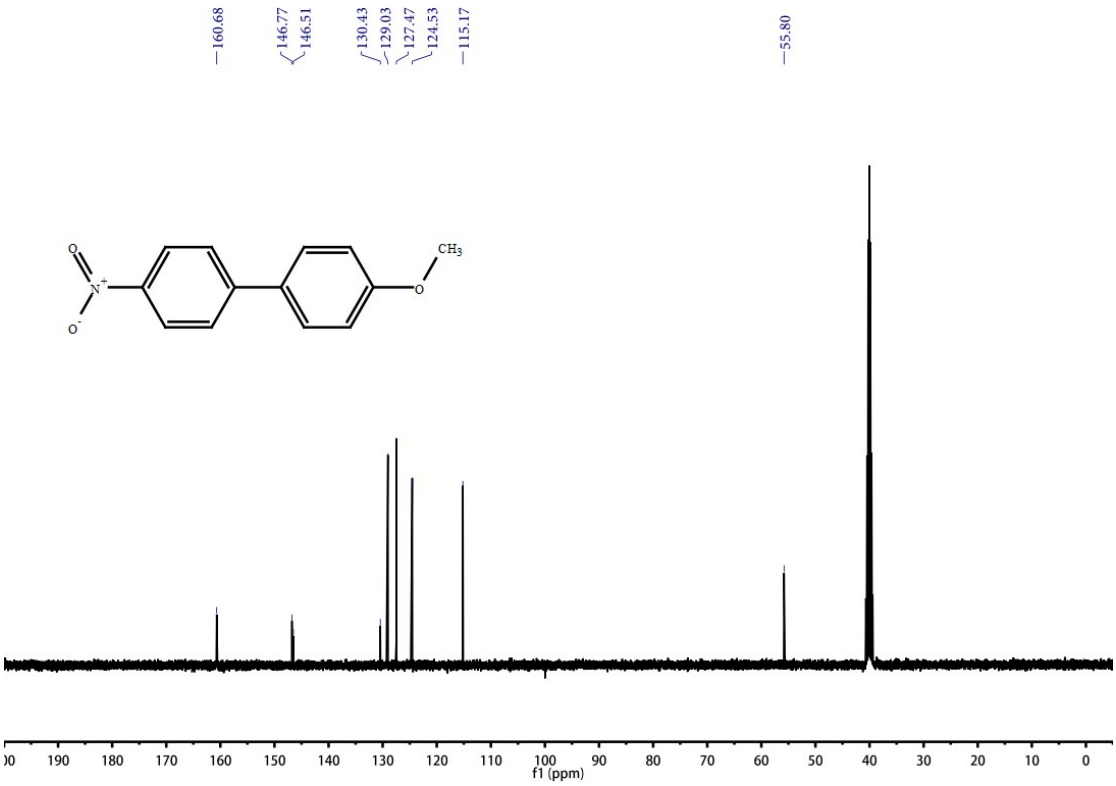

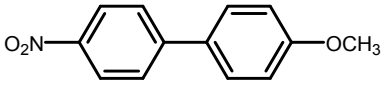

Fig. S22 4-methoxy-4'-nitro-1, 1'-biphenyl: ^{13}C NMR (100 MHz, dmso) 160.68, 146. 77, 146.51, 130.43, 129.03, 127.47, 124.53, 115.77, 55.80.

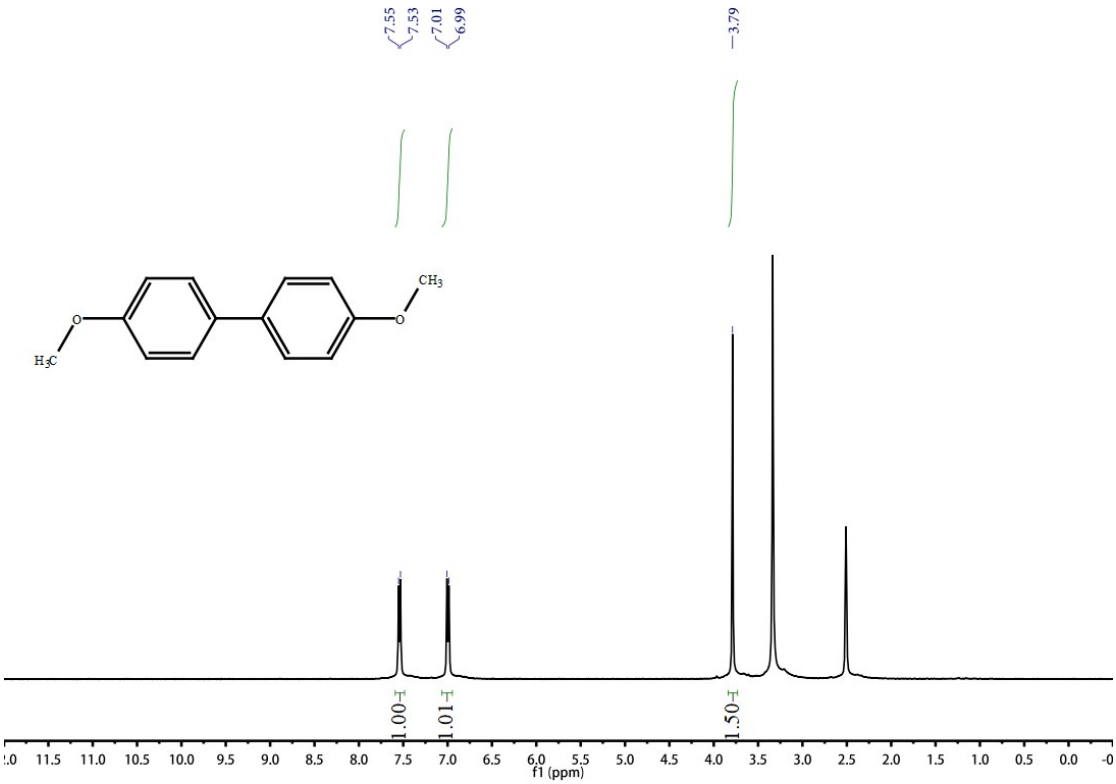

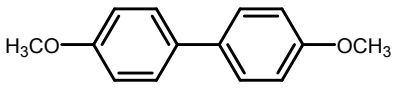

Fig. S23 4, 4'-dimethoxy-1,1'-biphenyl: ^{1}H NMR (400 MHz, dmso) 7.54 (d, J = 8.6 Hz, 4H), 7.00 (d, J = 8.6 Hz, 4H), 3.79 (s, 6H).

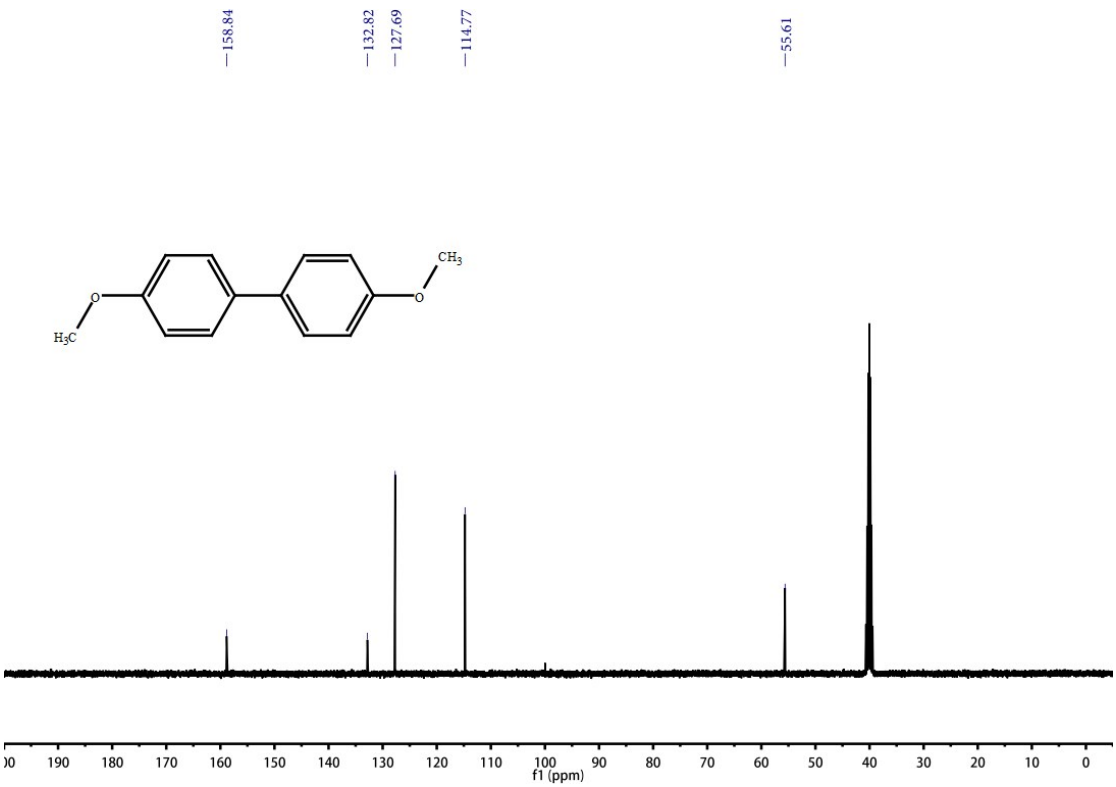

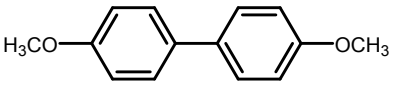

Fig. S24 4, 4'-dimethoxy-1,1'-biphenyl: ^{13}C NMR (100 MHz, dmso) 158.84, 132.82, 127.69, 114.77, 55.61.

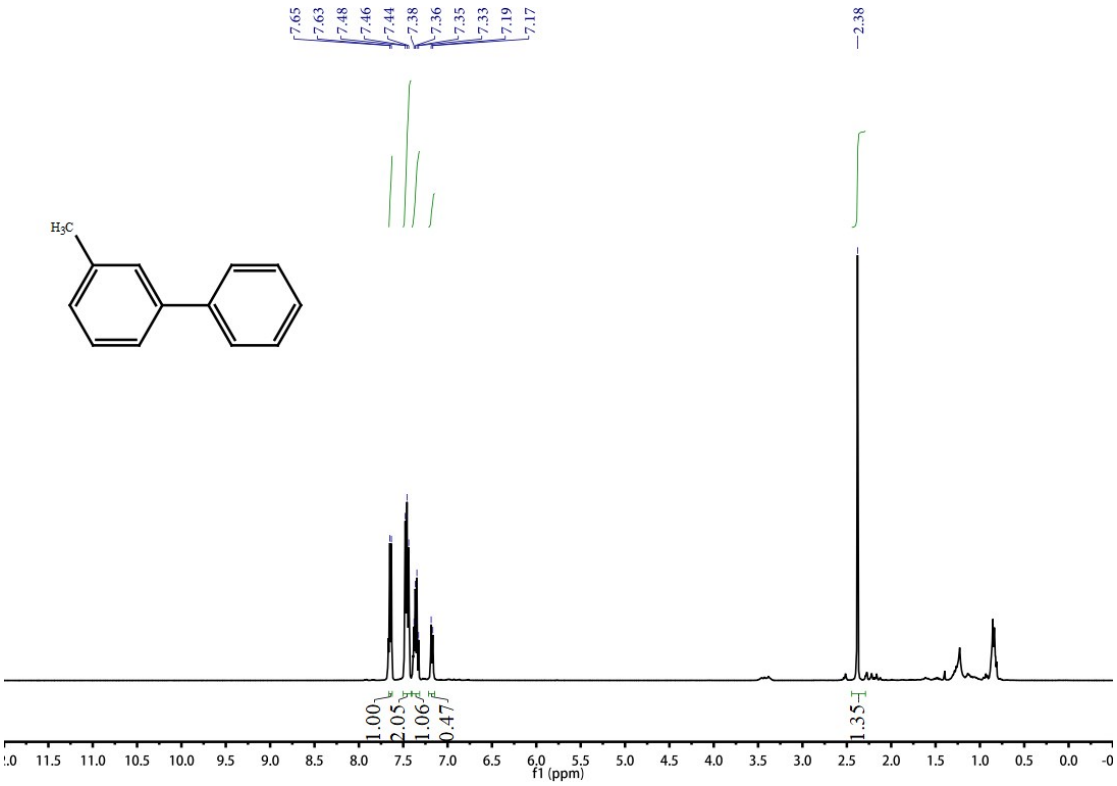

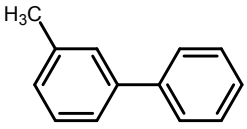

Fig. S25 3-Methyl-1,1-Biphenyl: ^{1}H NMR (400 MHz, dmso) 7.64 (d, *J* = 7.1 Hz, 2H), 7.46 (t, *J* = 7.6 Hz, 4H), 7.35 (dd, *J*=7.5 Hz, 2H), 7.18 (d, *J*=7.5 Hz, 1H), δ 2.38 (s, 3H).

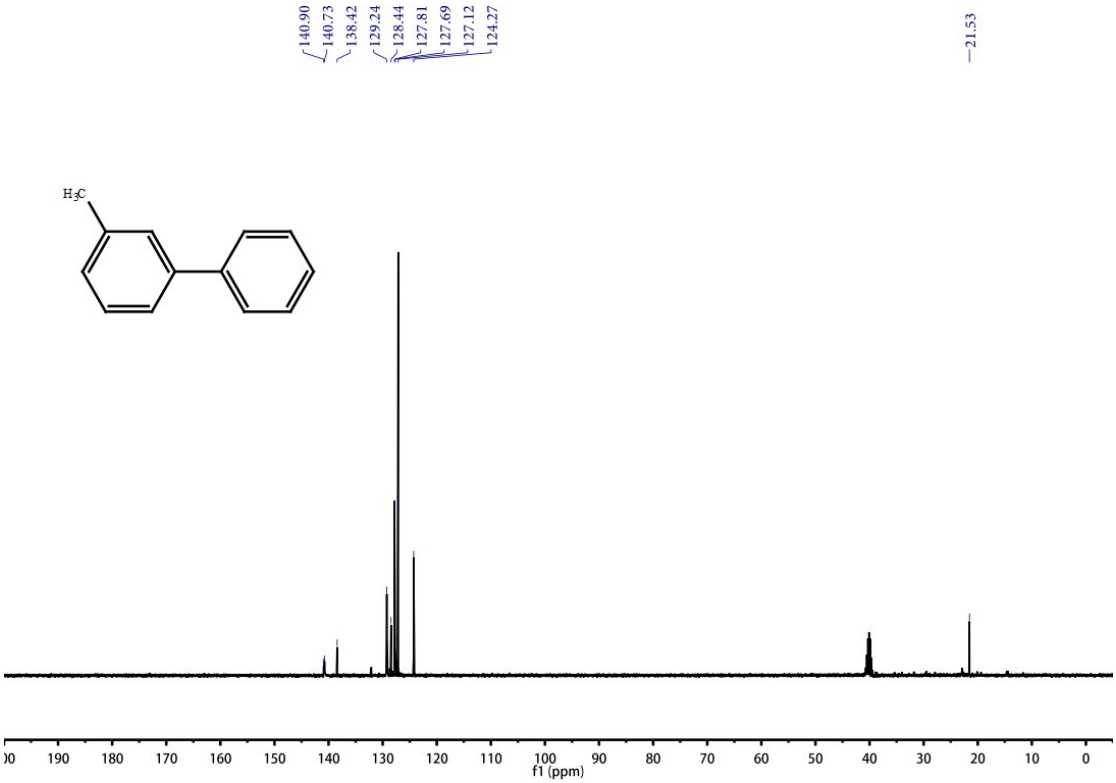

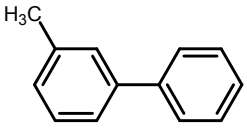

Fig. S26 3-Methyl-1,1-Biphenyl: ^{13}C NMR (100 MHz, dmso) 140.90, 140.73, 138.42, 129.24, 128.44, 127.81, 127.69, 127.12, 124.27, 21.53.

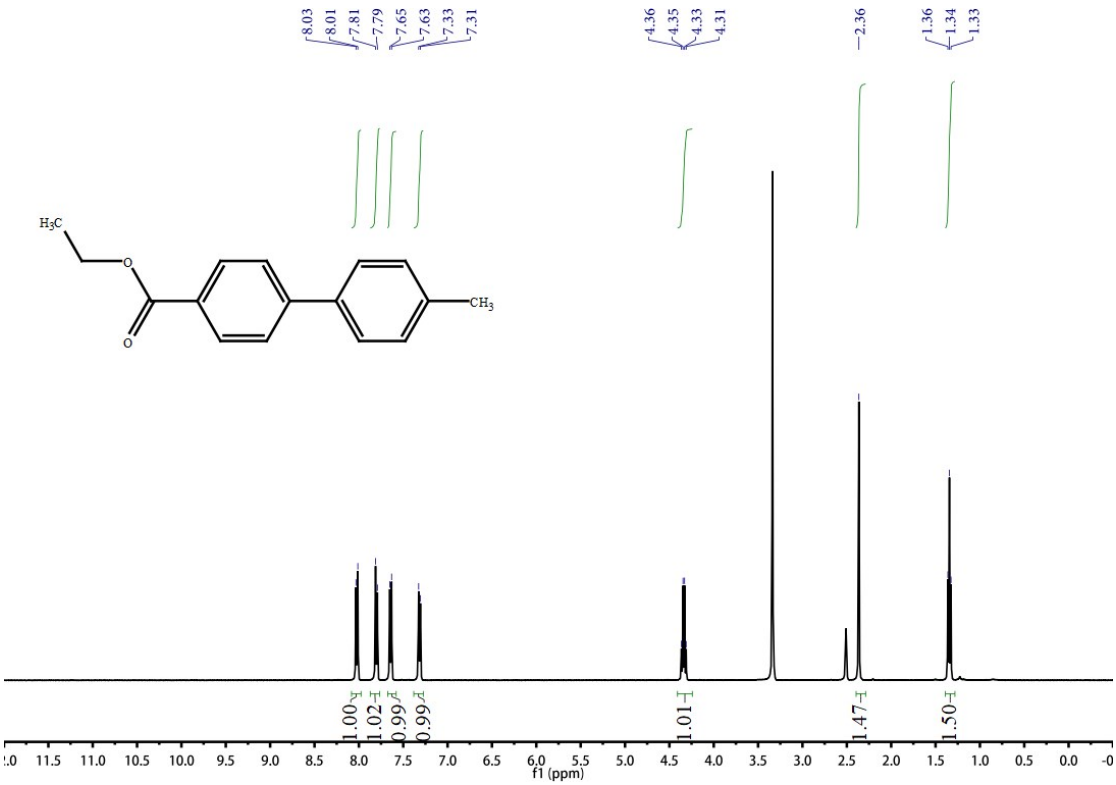

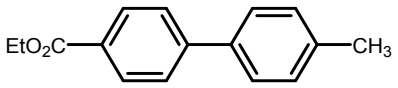

Fig. S27 ethyl 4'-methyl-[1,1'-biphenyl]-4-carboxylate: ^{1}H NMR (400 MHz, dmso) 8.02 (d, *J* = 8.4 Hz, 2 H), 7.80 (d, *J* = 8.3 Hz, 2H), 7.64 (d, *J* = 8. 1Hz, 2H), 7.32(d, *J* = 8.1 Hz, 2H), 4.33 (q, *J* = 7.1 Hz, 2H), 2.36 (s, 3H), 2.34 (t, *J* = 7.1 Hz, 3H).

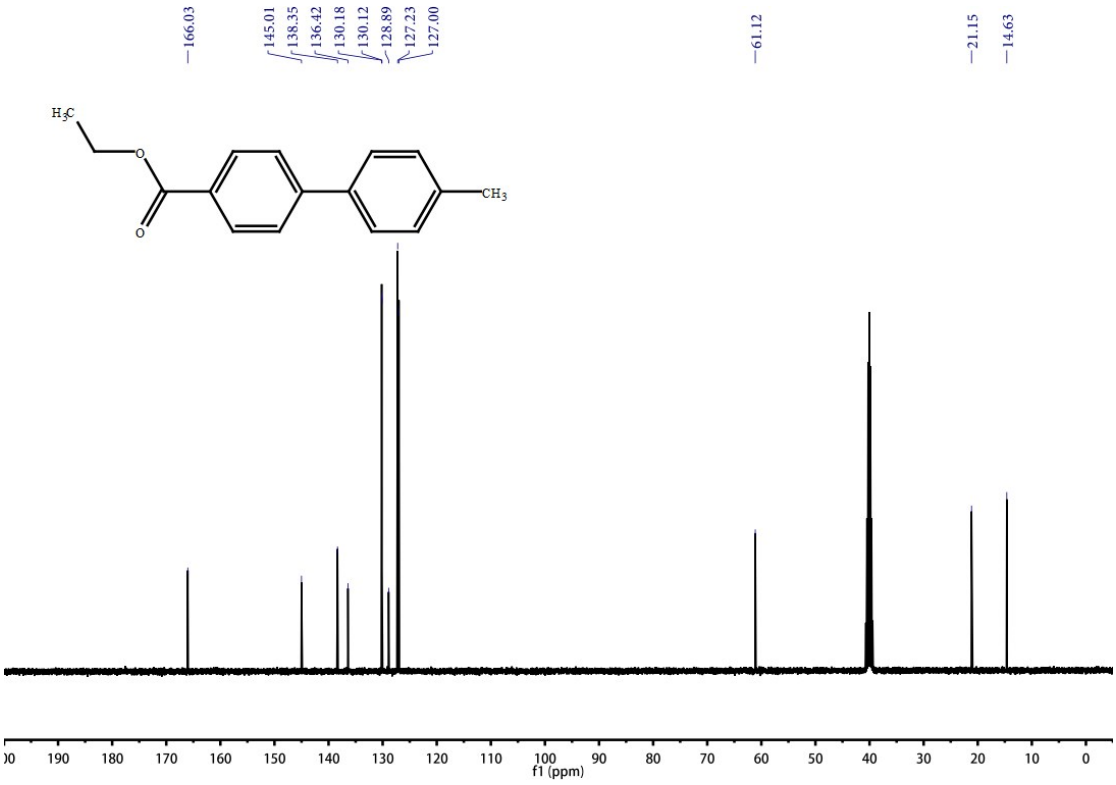

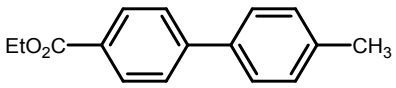

Fig. S28 ethyl 4'-methyl-[1,1'-biphenyl]-4-carboxylate: ^{13}C NMR (100 MHz, dmso) 166.03, 145.01, 138.35, 136.42, 130.18, 128.89, 127.23, 127. 00, 61.12, 21.15, 14.63.

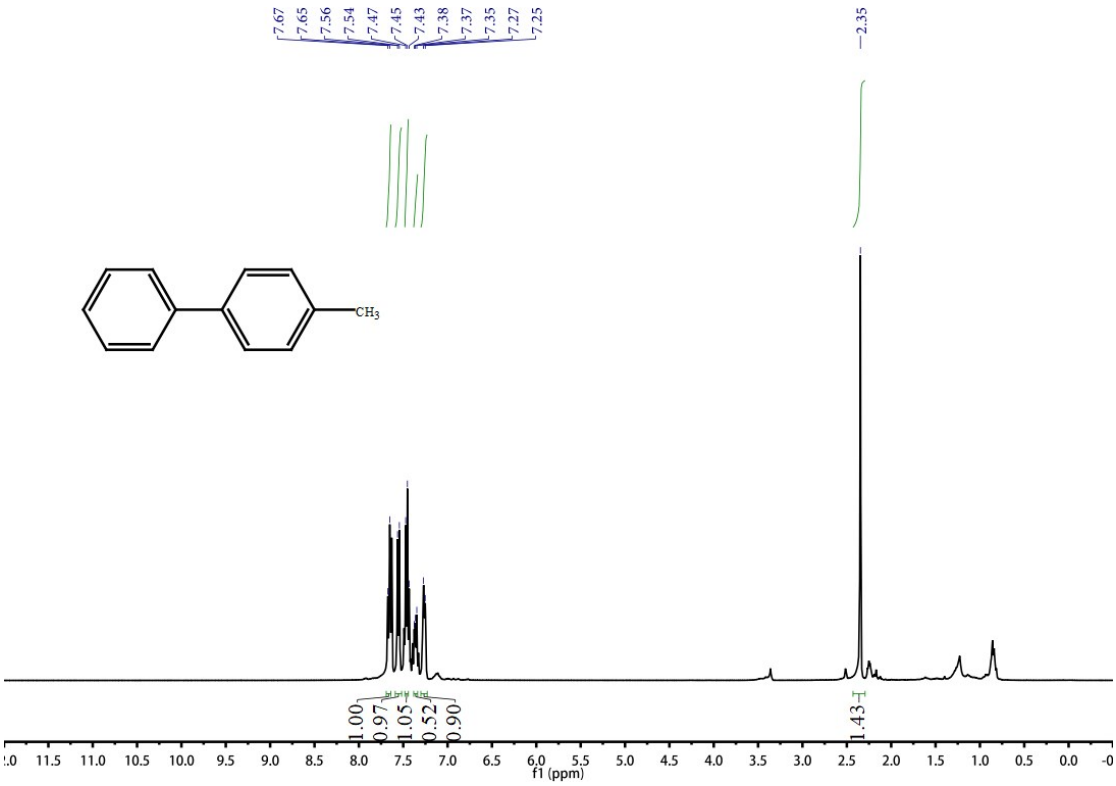

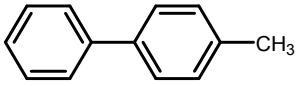

Fig. S29 4-methyl-1,1'-biphenyl: ^{1}H NMR (400 MHz, dmso) 7.66 (d, *J* = 8.4 Hz, 2H), 7.55 (d, *J* = 8.1 Hz, 2H), 7.46 (t, *J* = 7.8, 2H), 7.37 (t, *J* = 7.4 Hz, 1H), 7.26 (d, *J* = 7.6 Hz, 1H), 2.35 (s, 3H).

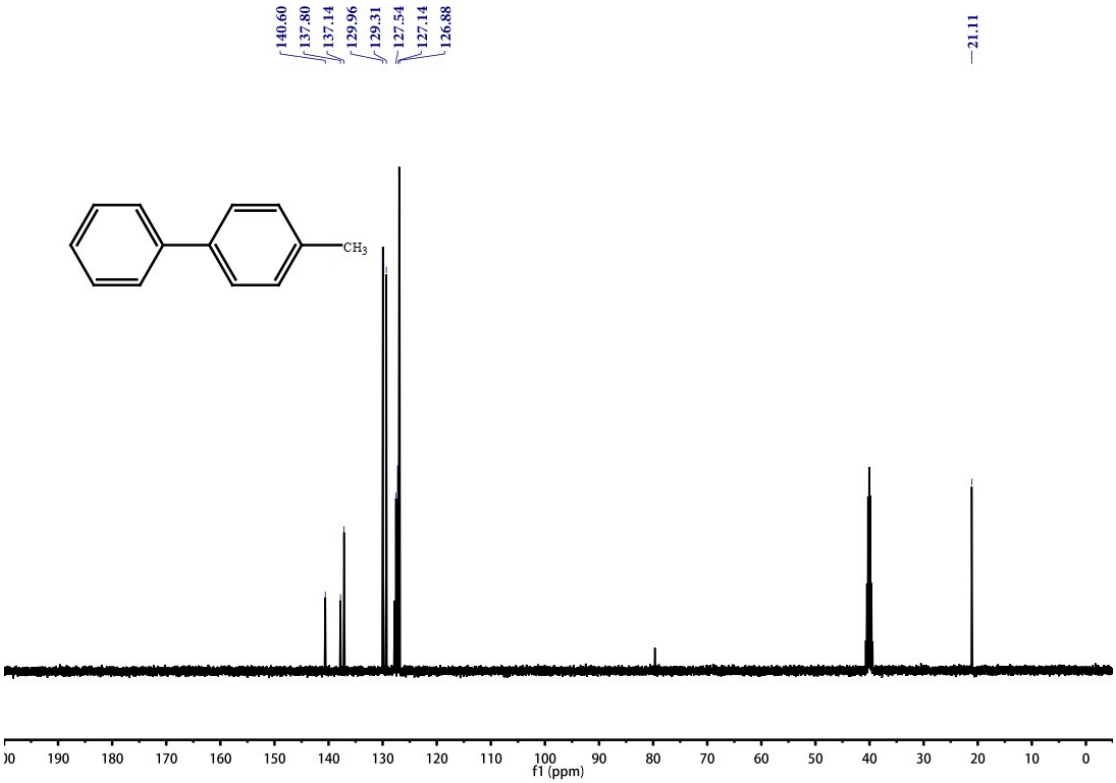

Fig. S30 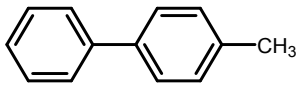

4-methyl-1,1'-biphenyl: ^{13}C NMR(100 MHz, dmso) 140.60, 137.80, 137.14, 129.96, 129.31, 127.54, 127.14, 126.88, 21.11.

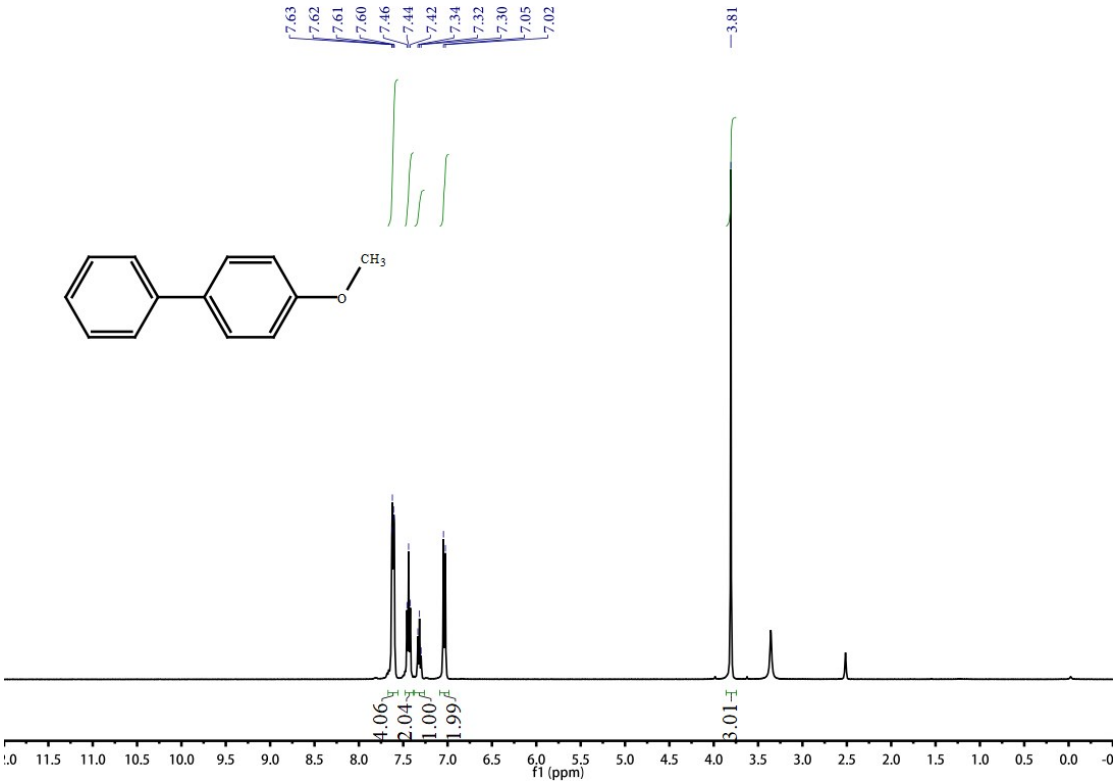

Fig. S31 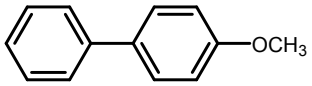

4-methoxy-1,1'-biphenyl: ^{1}H NMR (400 MHz, dmso): 7.61 (dd, J = 8.2, 2.7 Hz, 4H), 7.44 (t, J = 7.6 Hz, 2H), 7.32 (t, J = 7.3 Hz, 1H), 7.03 (d, J = 8.7 Hz, 2H), 3.81 (s, 3H).

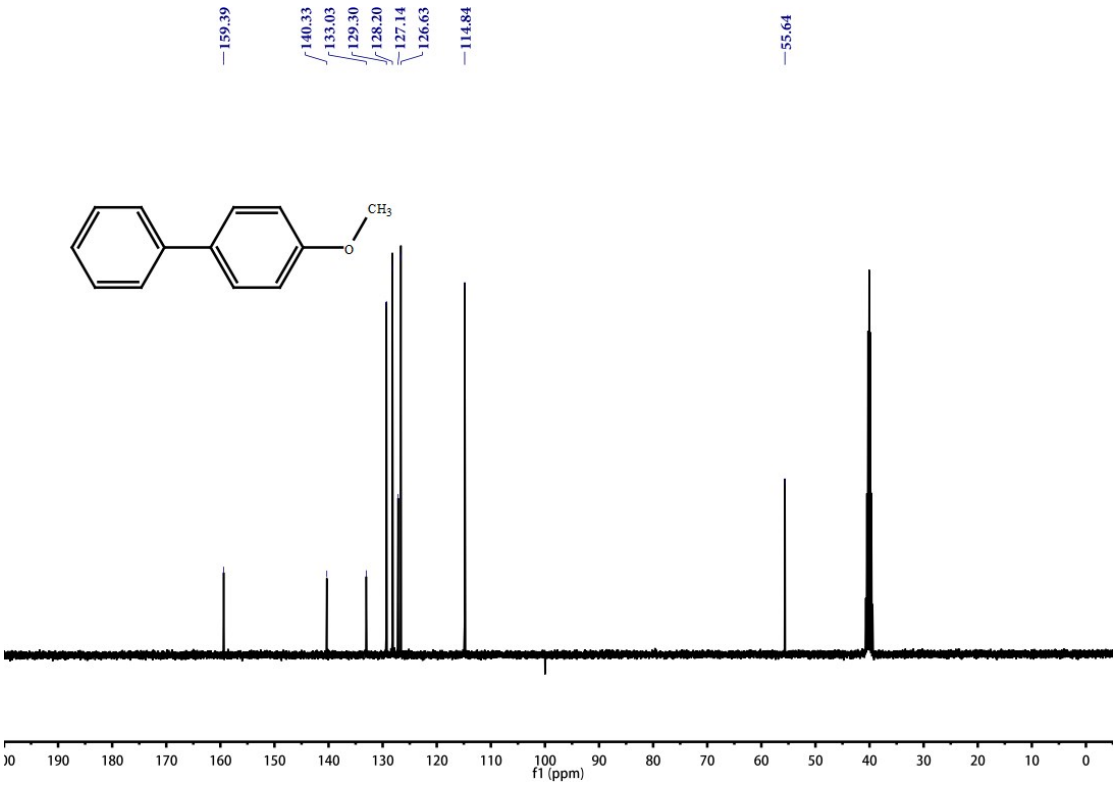

Fig. S32 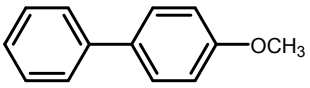

4-methoxy-1,1'-biphenyl: ^{13}C NMR (100 MHz, dmso) 159.39, 140.33, 133.03, 129.30, 128.20, 127.14, 126.63, 114.84, 55.64.

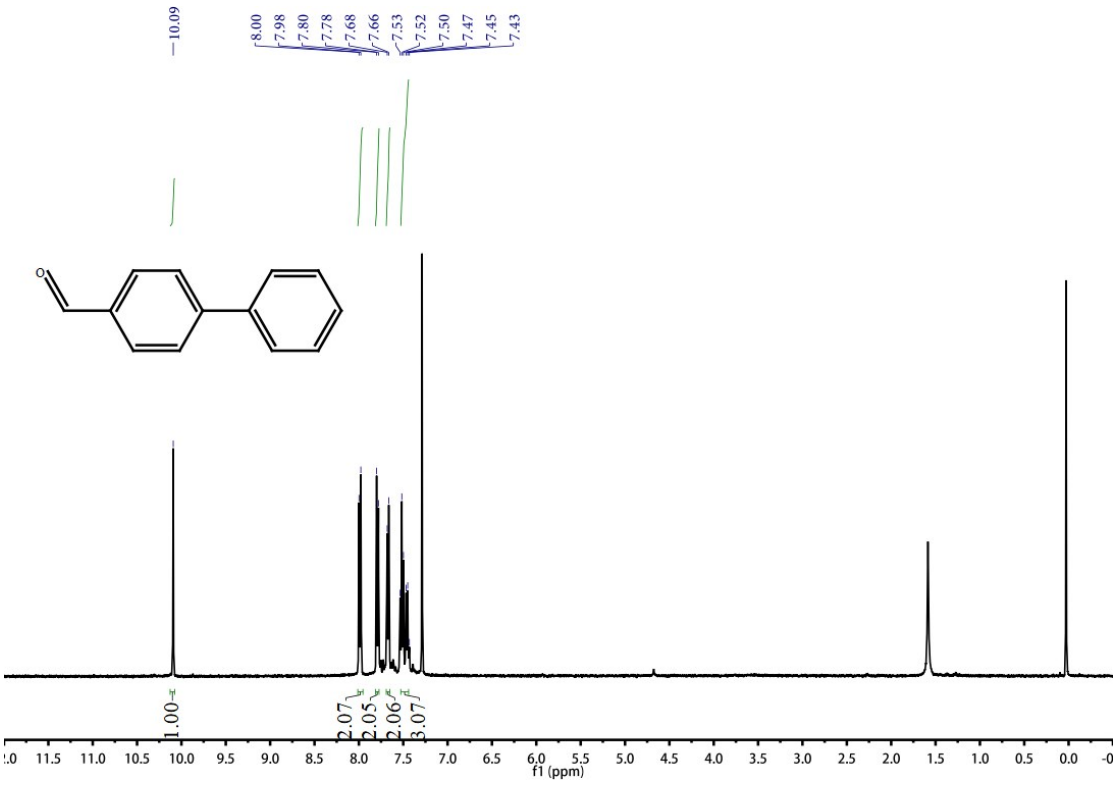

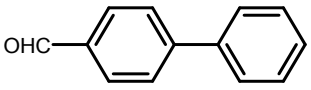

Fig. S33 [1,1'-biphenyl]-4-carbaldehyde: ^{1}H NMR (400 MHz, CDCl3) 10.09 (s, 1H), 7.99 (d, J = 8.3 Hz, 2H), 7.79 (d, J = 8.3 Hz, 2H), 7.67 (d, J = 7.0 Hz, 2H), 7.48 (dd, J = 19.4, 7.4 Hz, 2H), 7.45 (dd, J = 19.4, 7.4 Hz, 3H).

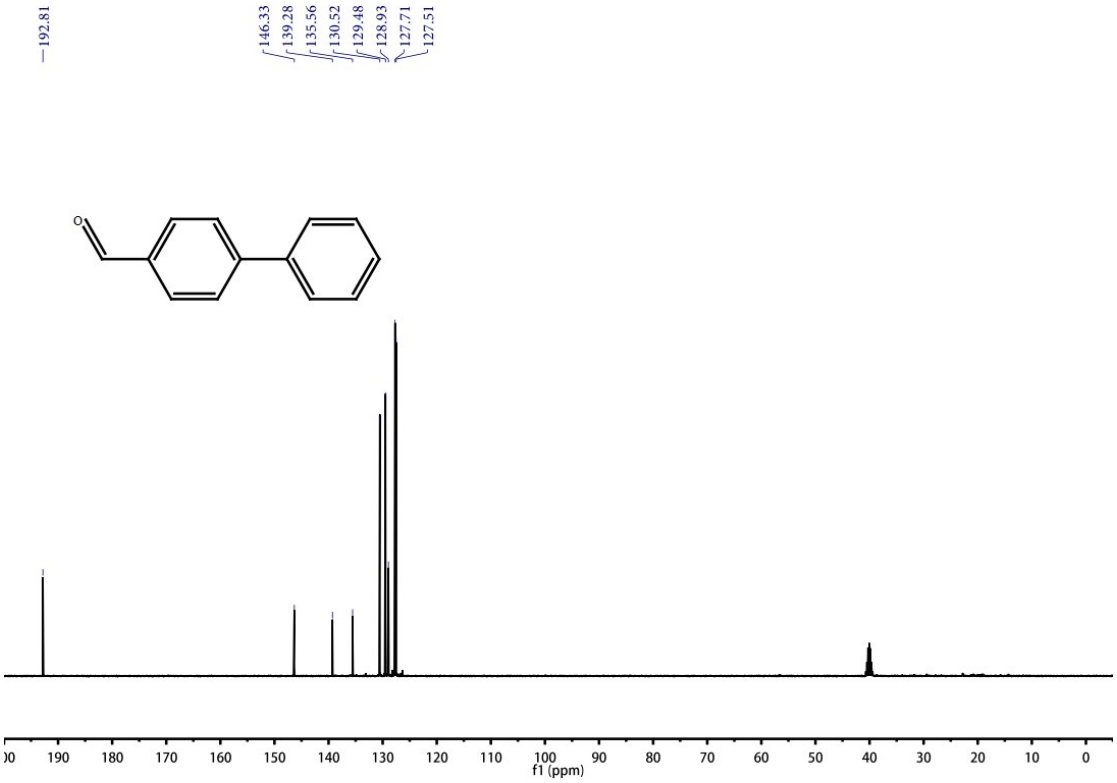

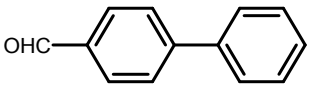

Fig. S34 [1,1'-biphenyl]-4-carbaldehyde: ^{13}C NMR (100 MHz, $CDCl_3$) 192.81, 146.33, 139.28, 135.56, 130.52, 129.48, 128.93, 127.71, 127.51.

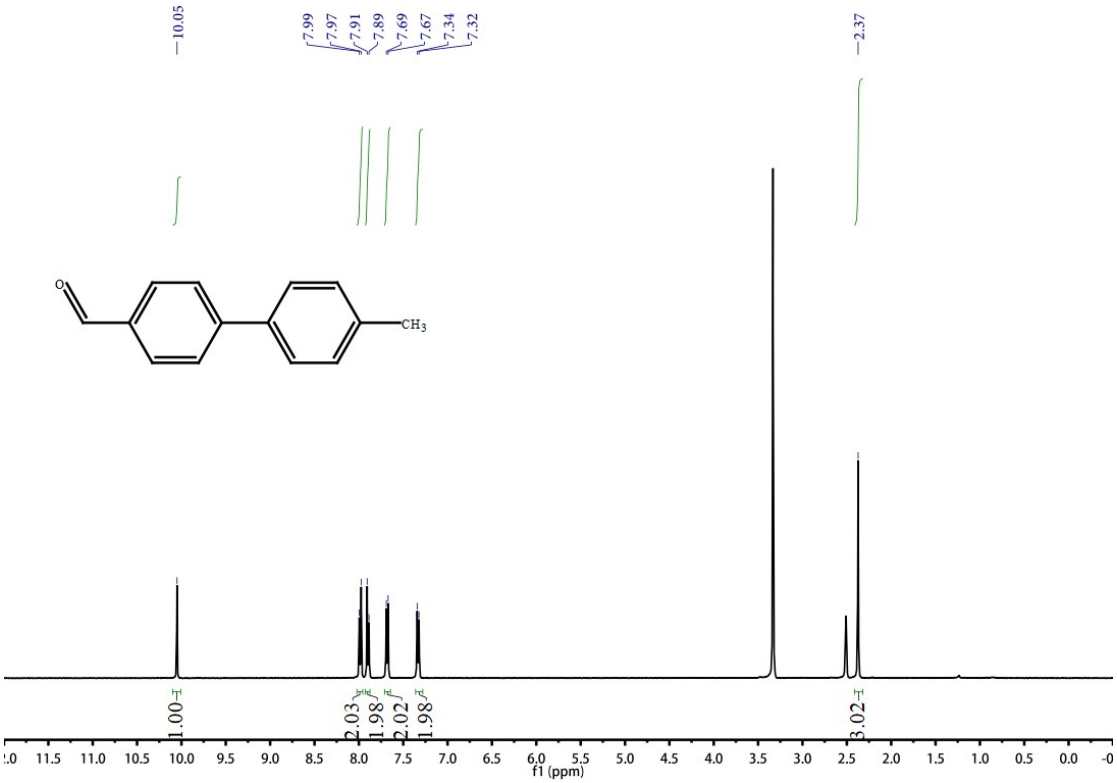

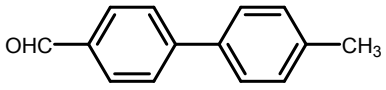

Fig. S35 4'-methyl-[1,1'-biphenyl]-4-carbaldehyde: ^{1}H NMR (400 MHz, dmso): 10.05 (s, 1H), 7.98 (d, J = 8.2 Hz, 2H), 7.90 (d, J = 8.2 Hz, 2H), 7.68 (d, J = 8.1 Hz, 2H), 7.33 (d, J = 8.1 Hz, 2H), 2.37 (s, 3H).

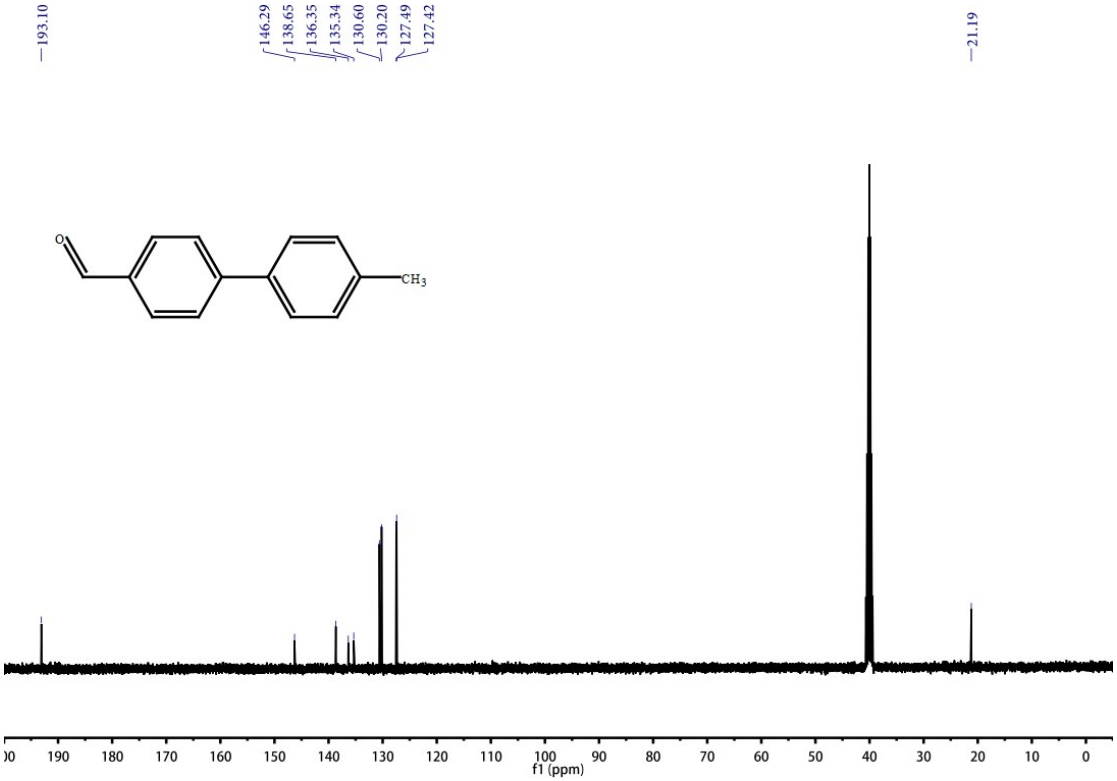

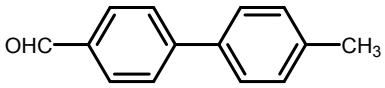

Fig. S36 4'-methyl-[1,1'-biphenyl]-4-carbaldehyde:^{13}C NMR (100 MHZ, dmso) 193.10, 146.29, 138.65, 136.35, 135.34, 130.60, 130.20, 127.49, 127.42, 21.19.

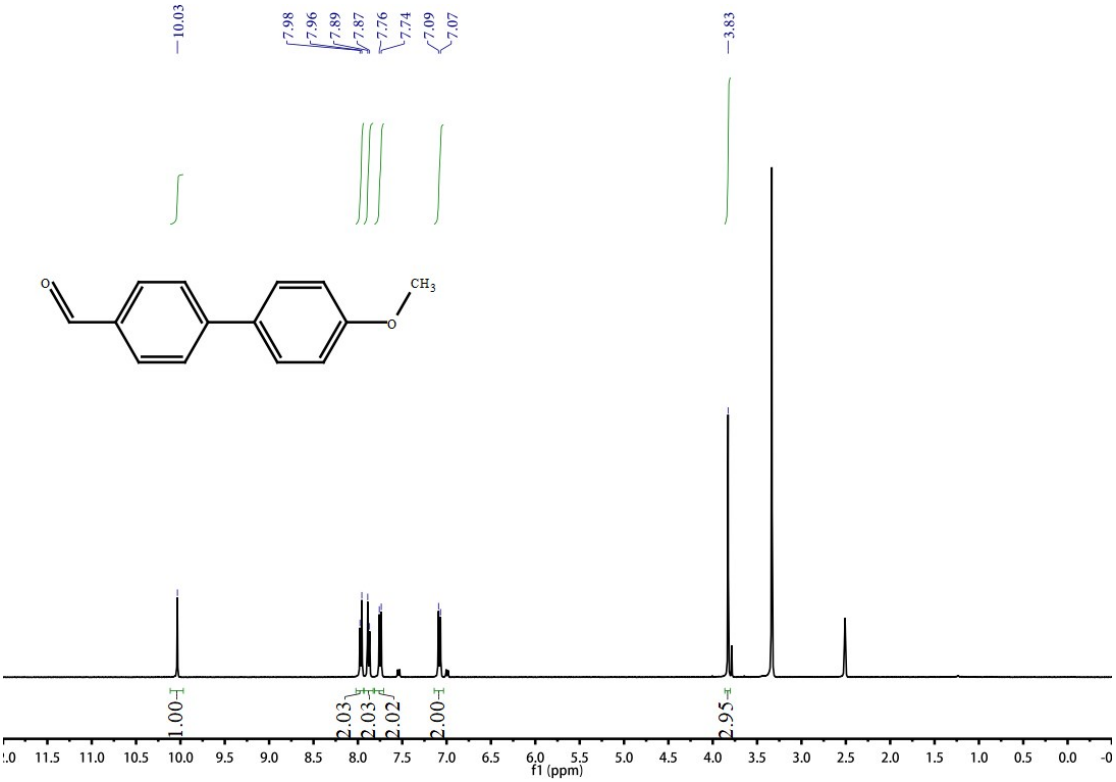

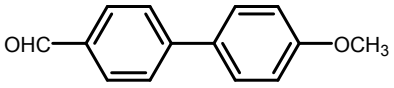

Fig. S37 4'-methoxy-[1,1'-biphenyl]-4-carbaldehyde: ^{1}H NMR (400MHz, dmso) 10.03 (s, 1H), 7.97 (d, *J* = 8.4 Hz, 2H), 7.88 (d, *J* = 8.3 Hz, 2H), 7.75 (d, *J* = 8.8 Hz, 2H), 7.08 (d, *J* = 8.8 Hz, 2H), 3.83 (s, 3H).

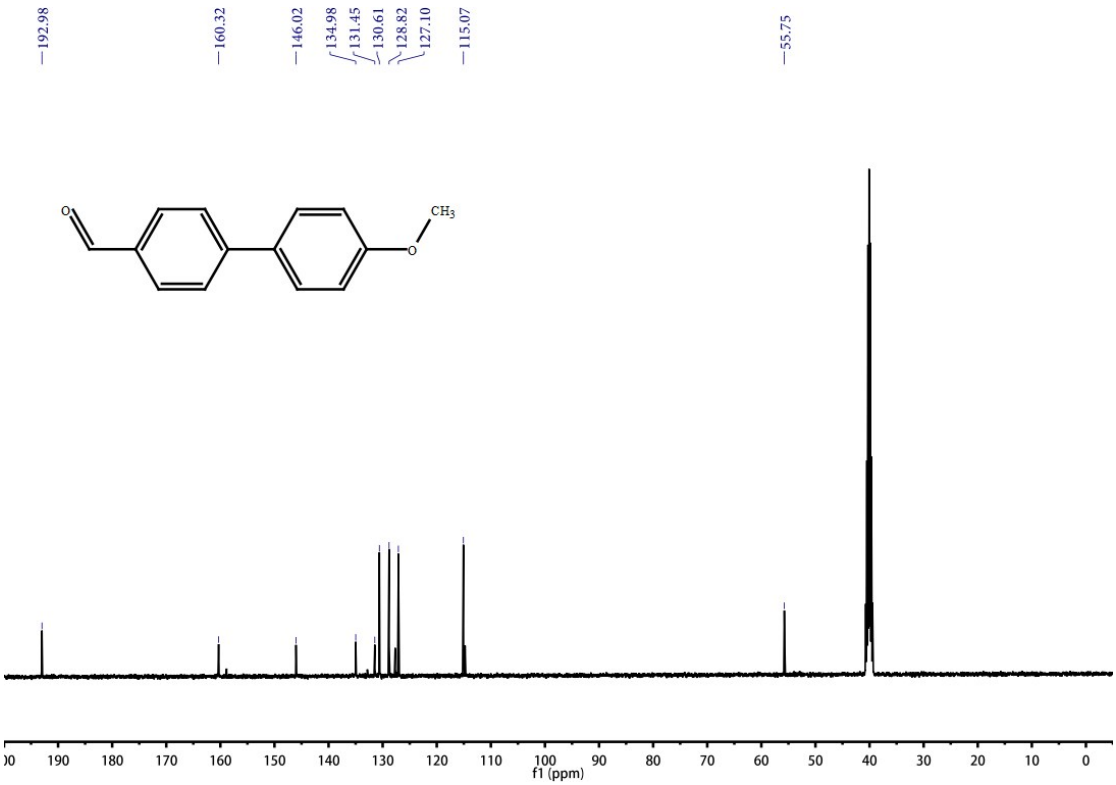

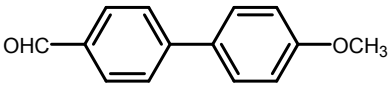

Fig. S38 4'-methoxy-[1,1'-biphenyl]-4-carbaldehyde: ^{13}C NMR (100 MHZ, dmso) 192.98, 160.32, 146.02, 134.98, 131.45, 130.61, 128.82, 127.10, 115.07, 55.75.

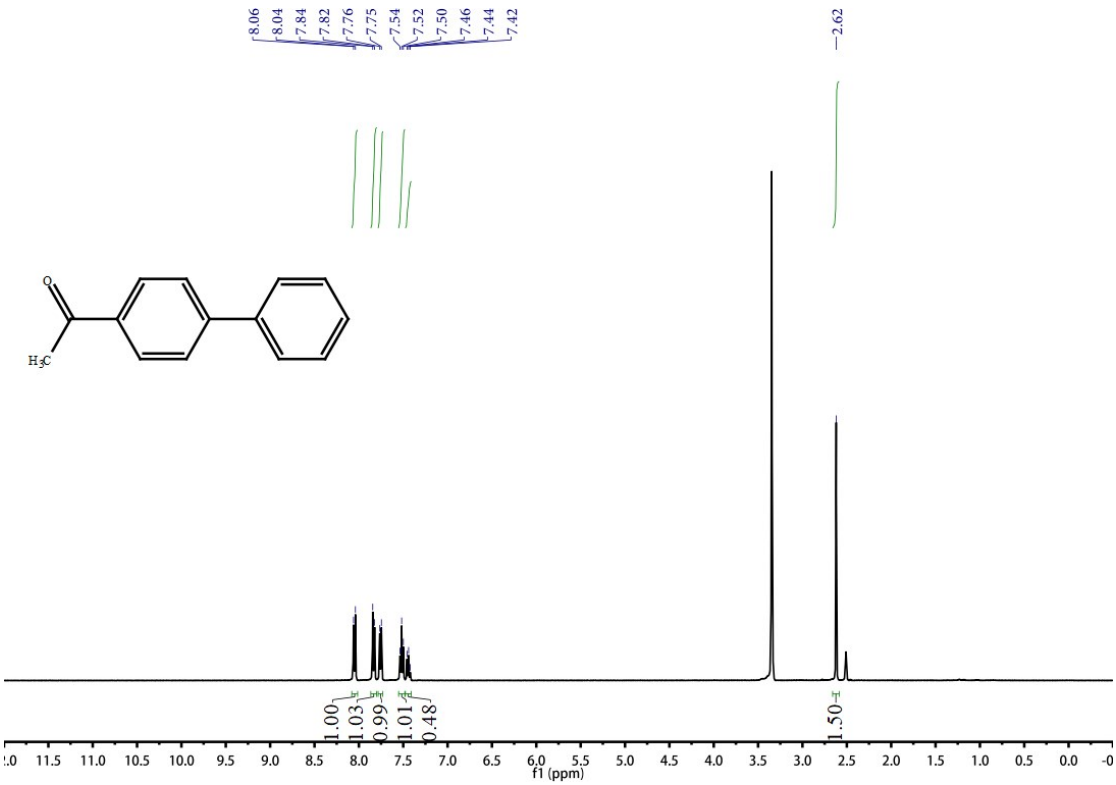

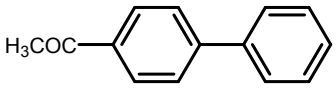

Fig. S39 1-([1,1'-biphenyl]-4-yl)ethan-1-one: ^{1}H NMR (400 MHz, dmso): 8.05 (d, *J* = 8.5 Hz, 2H), 7.83 (d, *J* = 8.5 Hz, 2H), 7.75 (d, *J* = 7.1 Hz, 2H), 7.52 (t, *J* = 7.4 Hz, 2H), 7.44 (t, *J* = 7.3 Hz, 1H), 2.62 (s, 3H).

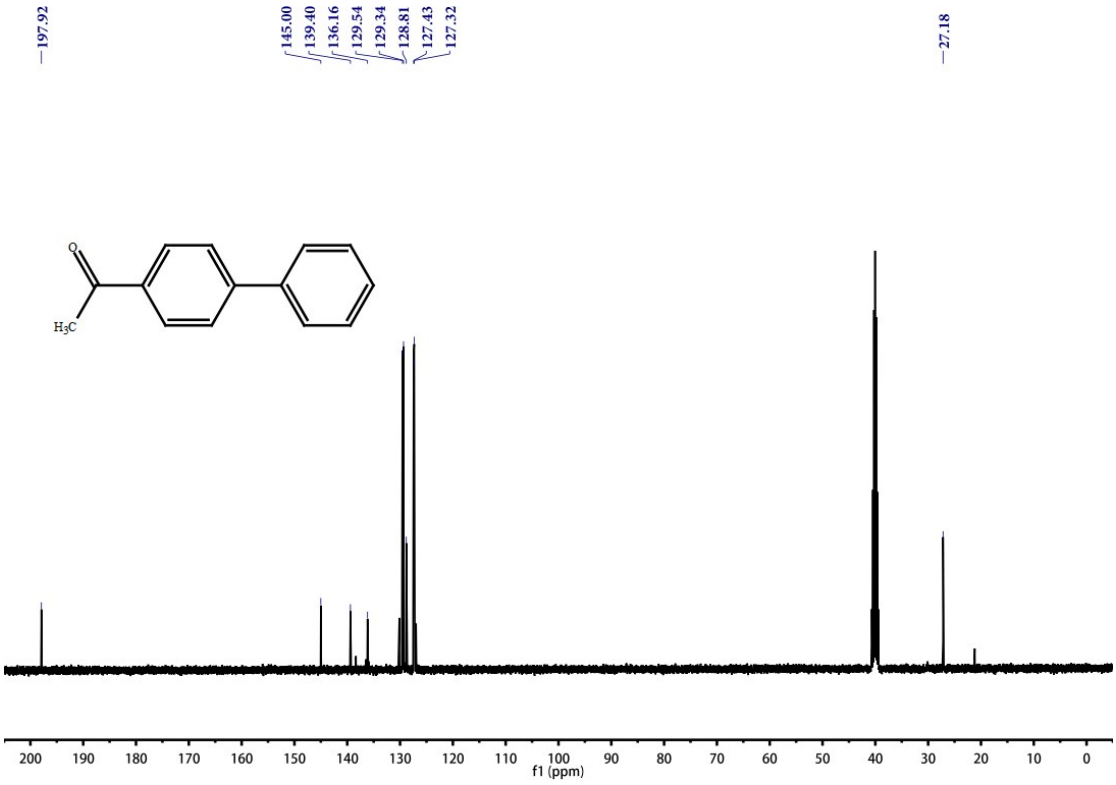

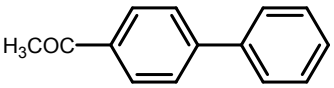

Fig. S40 1-([1,1'-biphenyl]-4-yl)ethan-1-one: ^{13}C NMR (100 MHz, dmso) 197.92, 145.00, 139.40, 136.16, 129.54, 129.34, 128.81, 127.43, 127.32, 27.18.

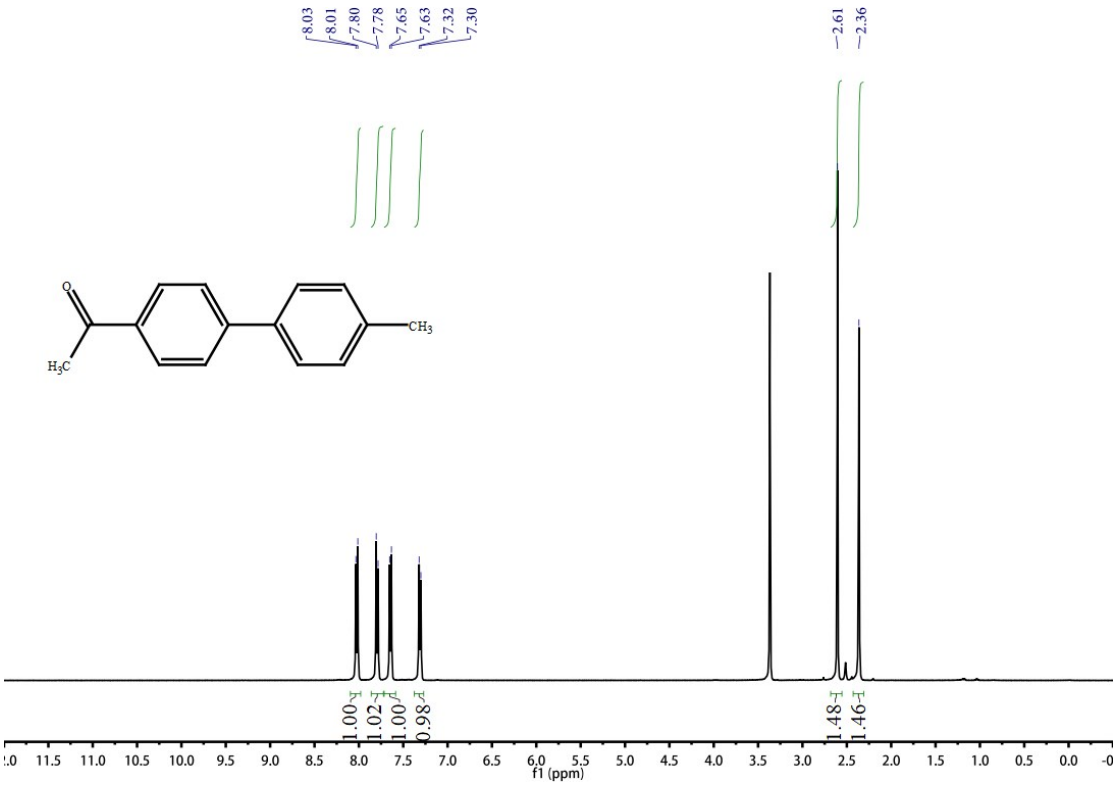

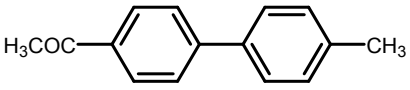

Fig. S41 1-(4'-methyl-[1,1'-biphenyl]-4-yl)ethan-1-one: ^{1}H NMR (400 MHz, dmso): 8.02 (d, *J* = 8.6 Hz, 2H), 7.79 (d, *J* = 8.6 Hz, 2H), 7.64 (d, *J* = 8.1 Hz, 2H), 7.31 (d, *J* = 7.9 Hz, 2H), 2.61 (s, 3H) 2.36 (s, 3H).

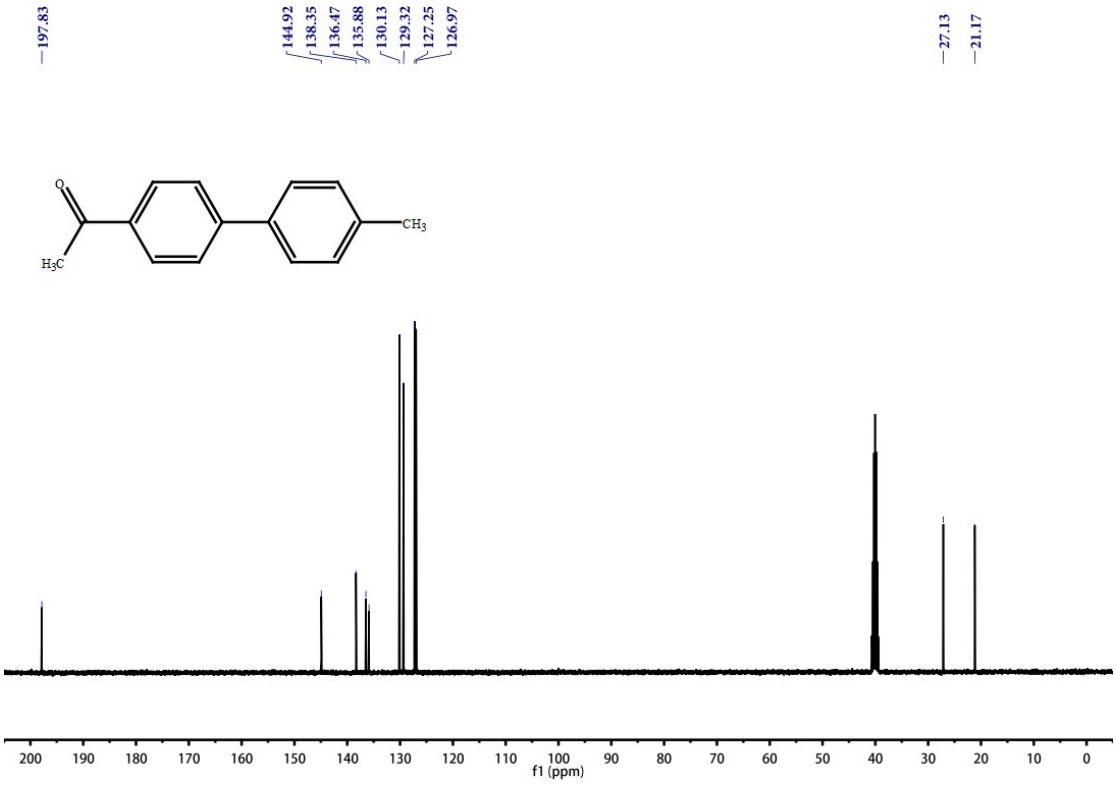

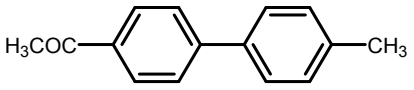

Fig. S42 1-(4'-methyl-[1,1'-biphenyl]-4-yl)ethan-1-one: ^{13}C NMR (100 MHz, dmso) 197.83, 144.92, 138.35, 136.47, 135.88, 130.13, 129.32, 127.25, 126.97, 27.13, 21.17.

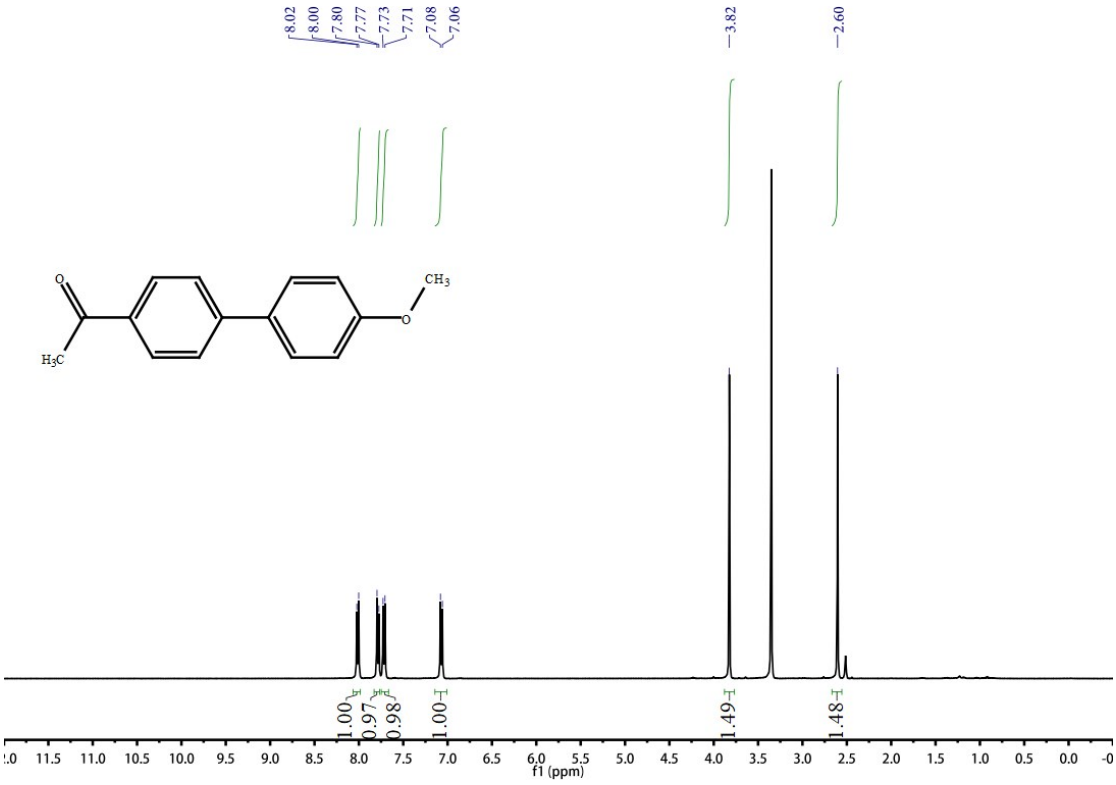

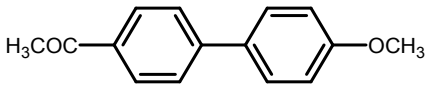

Fig. S43 1-(4'-methoxy-[1,1'-biphenyl]-4-yl)ethan-1-one: ^{1}H NMR (400 MHz, dmso), 8.01 (d, J = 8.6 Hz, 2H), 7.78 (d, J = 8.6 Hz, 2H), 7.72 (d, J = 8.9 Hz, 2H), 7.07 (d, J = 8.8 Hz, 2H), 3.82 (s, 3H), 2.60 (s, 3H).

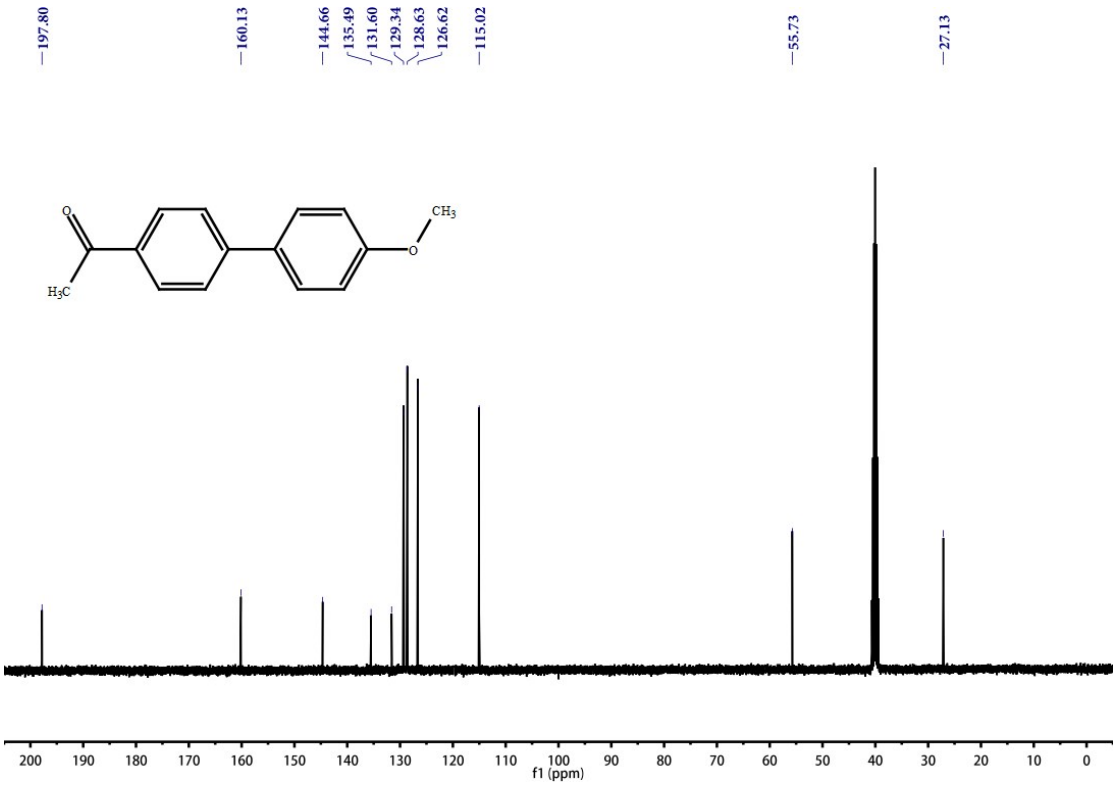

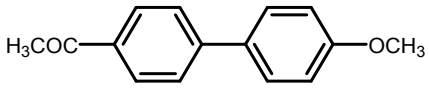

Fig. S44 1-(4'-methoxy-[1,1'-biphenyl]-4-yl)ethan-1-one:^{13}C NMR (100 MHz, dmso) 197.80, 160.13, 144.66, 135.49, 131.60, 129.34, 128.63, 126.62, 115.02, 55.73, 27.13.

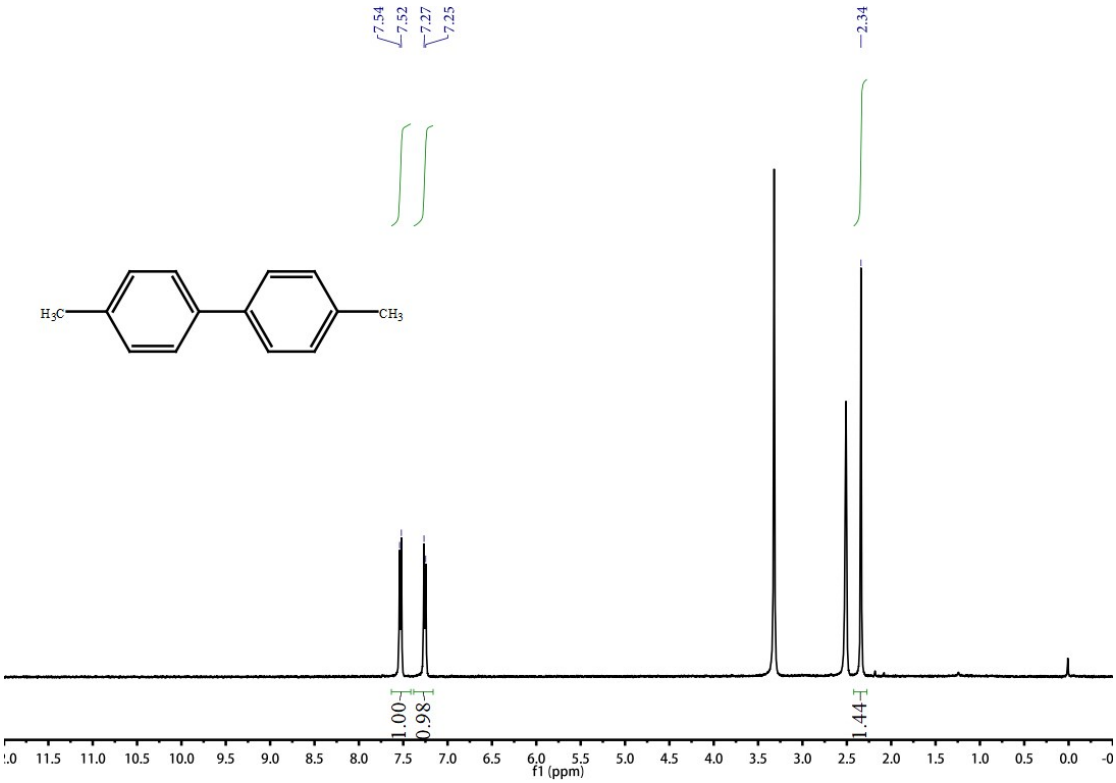

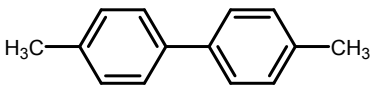

Fig. S45 4,4'-dimethyl-1,1'-biphenyl: ^{1}H NMR (400 MHz, dmso), 7.53 (d, J = 8.0 Hz , 4H), 7.26 (d, J = 7.8 Hz, 4H), 2.34 (s, 6H).

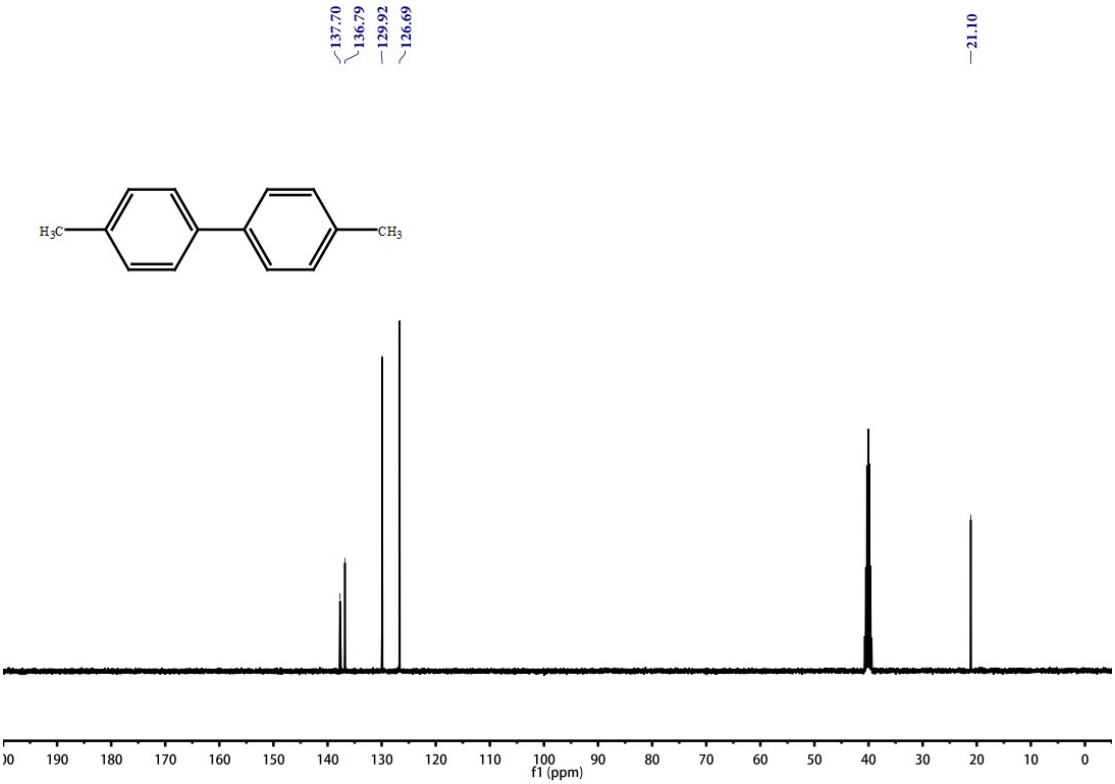

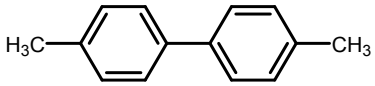

Fig. S46 4,4'-dimethyl-1,1'-biphenyl:^{13}C NMR (100 MHz, dmso) 137.70, 136.79, 129.92, 126.09, 22.10.

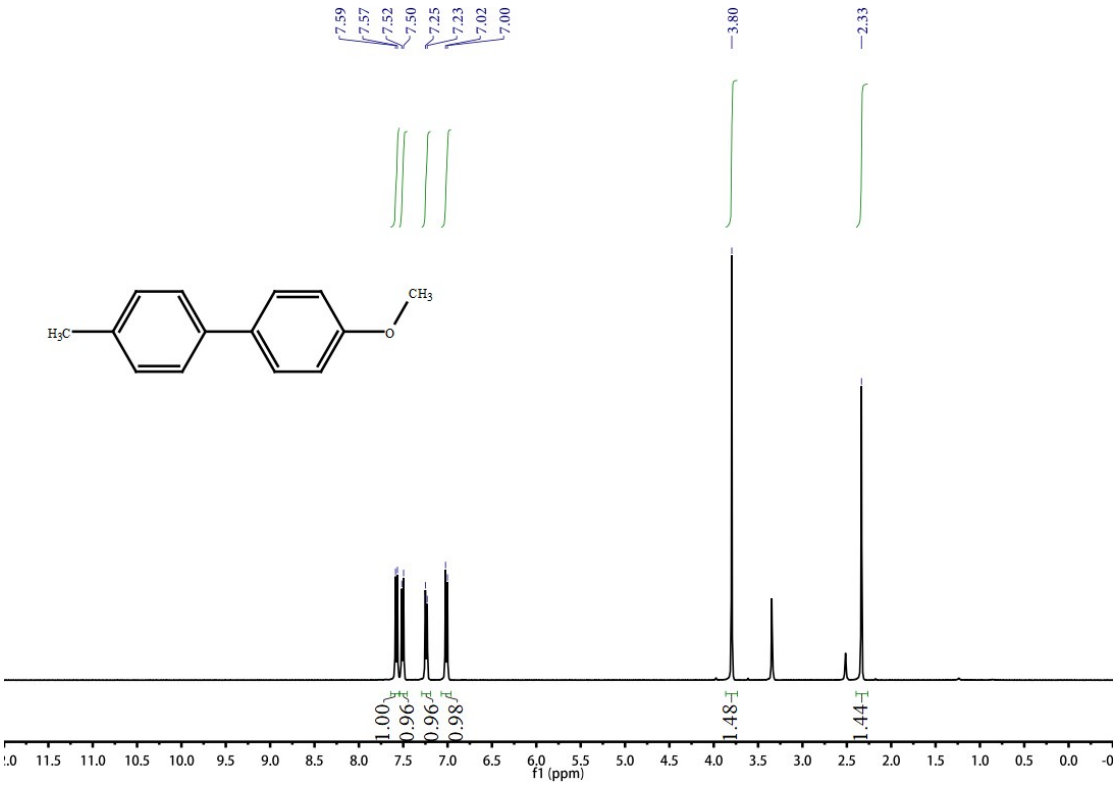

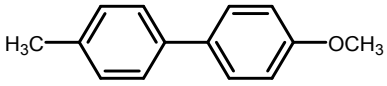

Fig. S47 4-methoxy-4'-methyl-1,1'-biphenyl: ^{1}H NMR (400 MHz, dmso): 7.58 (d, J = 8.7 Hz, 2H), 7.51 (d, J = 8.1 Hz, 2H), 7.24 (d, J = 8.2 Hz, 2H), 7.01 (d, J = 8.7 Hz, 2H), 3.80 (s, 3H).

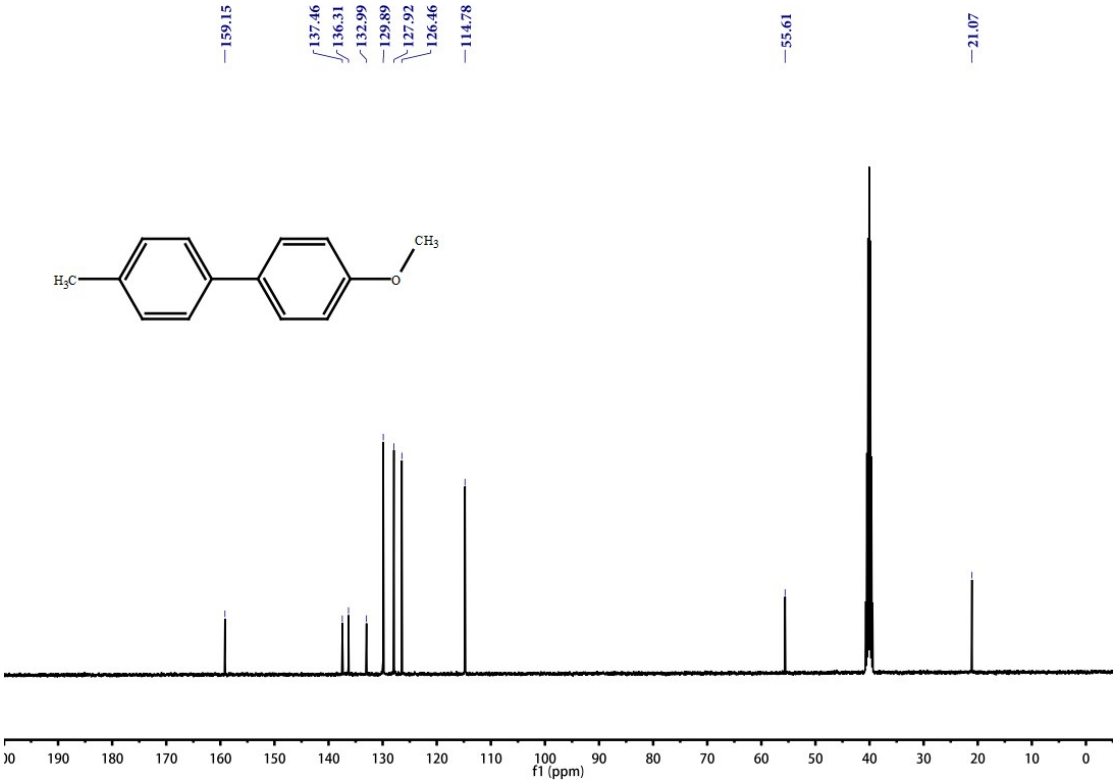

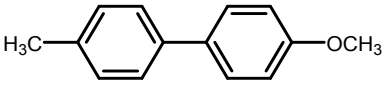

Fig. S48 4-methoxy-4'-methyl-1,1'-biphenyl: ^{13}C NMR (100 MHz, dmso) 159.15, 137.46, 136.31, 132.99, 129.89, 127.92, 126.46, 114.78, 55.61, 21.07.

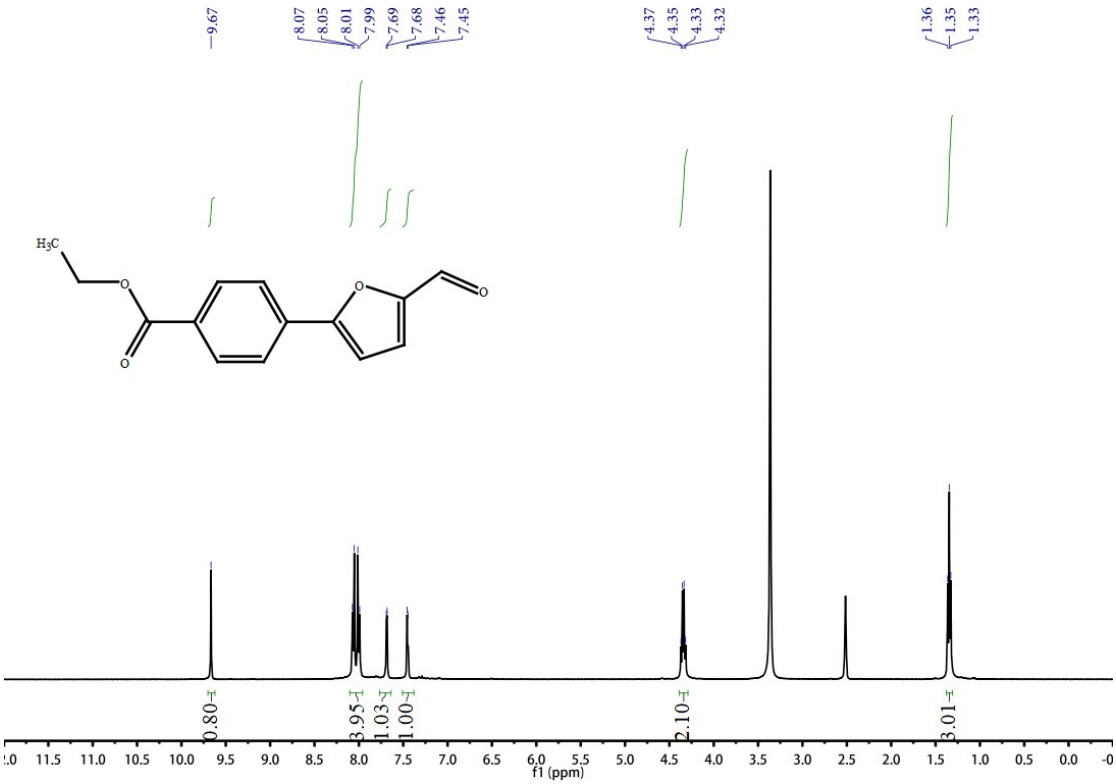

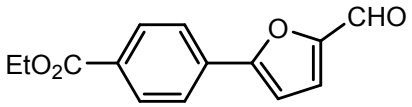

Fig. S49 ethyl 4-(5-formylfuran-2-yl)benzoate: ^{1}H NMR (400 MHz, dmso): δ 9.67 (s, 1H), 8.10-7.96 (m, 4H), 7.69 (d, *J* = 3.7 Hz, 1H), 7.45 (d, *J* = 3.7 Hz,1H), 4.34 (q, *J* = 7.1 Hz, 2H), 1.35 (t, *J* = 7.1 Hz, 3H).

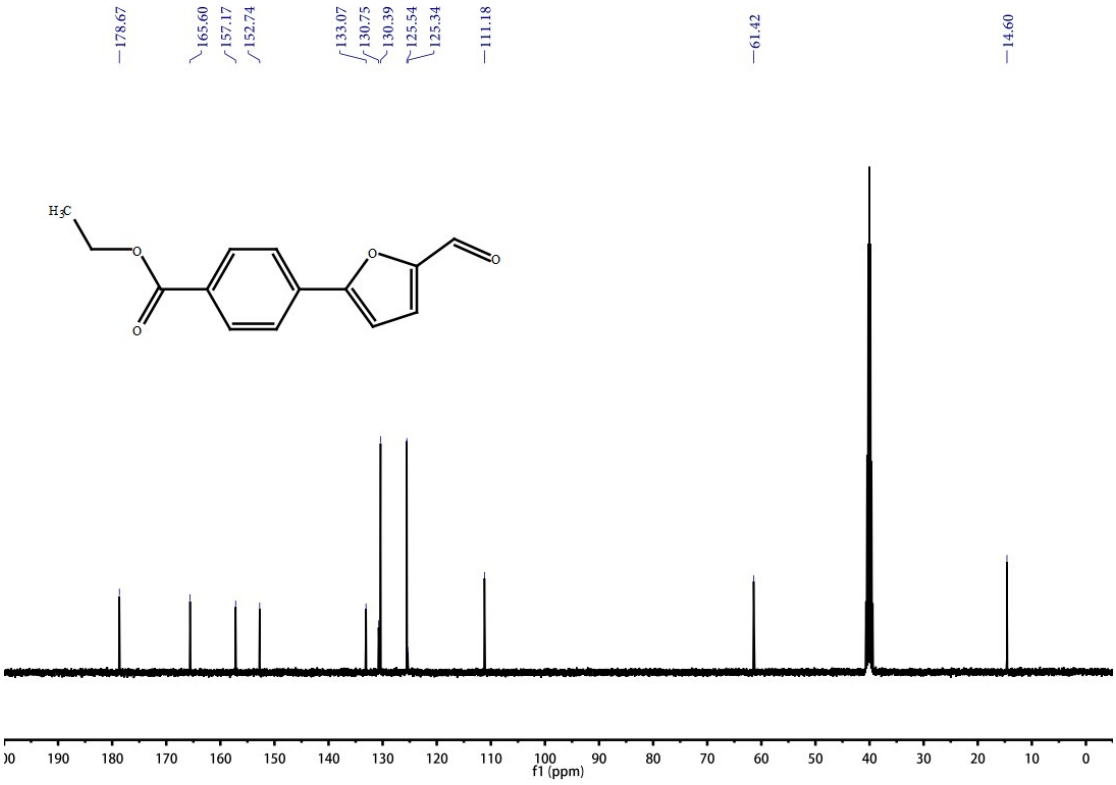

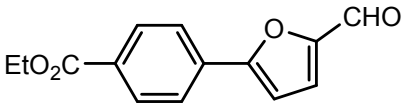

Fig. S50 ethyl 4-(5-formylfuran-2-yl)benzoate:^{13}C NMR (100 MHz, dmso) 178.67, 165.60, 157.17, 152.74, 133.07, 130.75, 125.54, 125.34, 111.18, 61.42, 14.60.

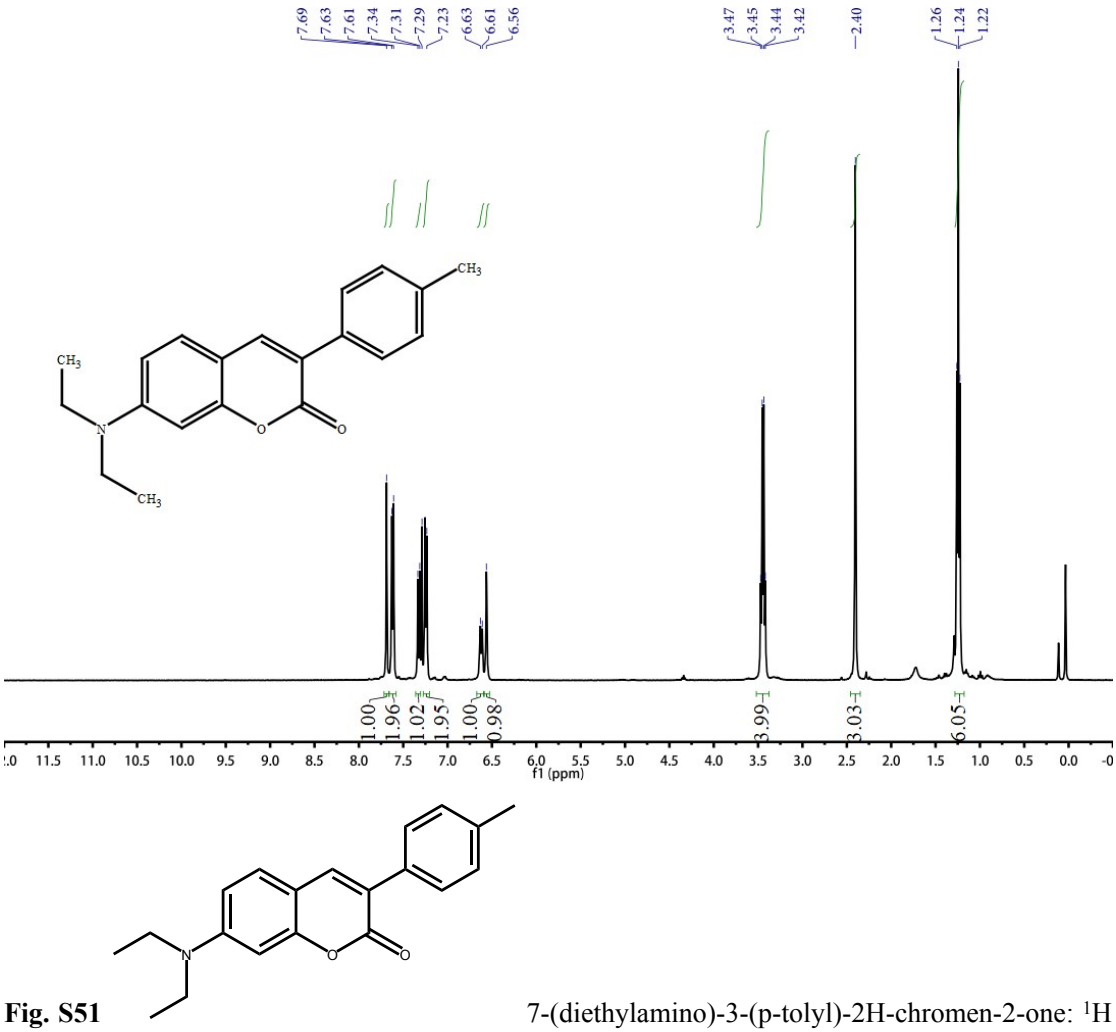

Fig. S51 7-(diethylamino)-3-(p-tolyl)-2H-chromen-2-one: ^{1}H NMR (400 MHz, $CDCl_3$), 7.69 (s, 1H), 7.62 (d, J = 8.1 Hz, 2H), 7.31 (s, 1H), 7.23 (s, 2H), 6.62 (d, J = 8.7 Hz, 2H), 6.56 (s, 1H); 3.45 (q, J = 7.0 Hz, 4H), 2.40 (s, 3H), 1.24 (t, J = 7.1 Hz, 6H).

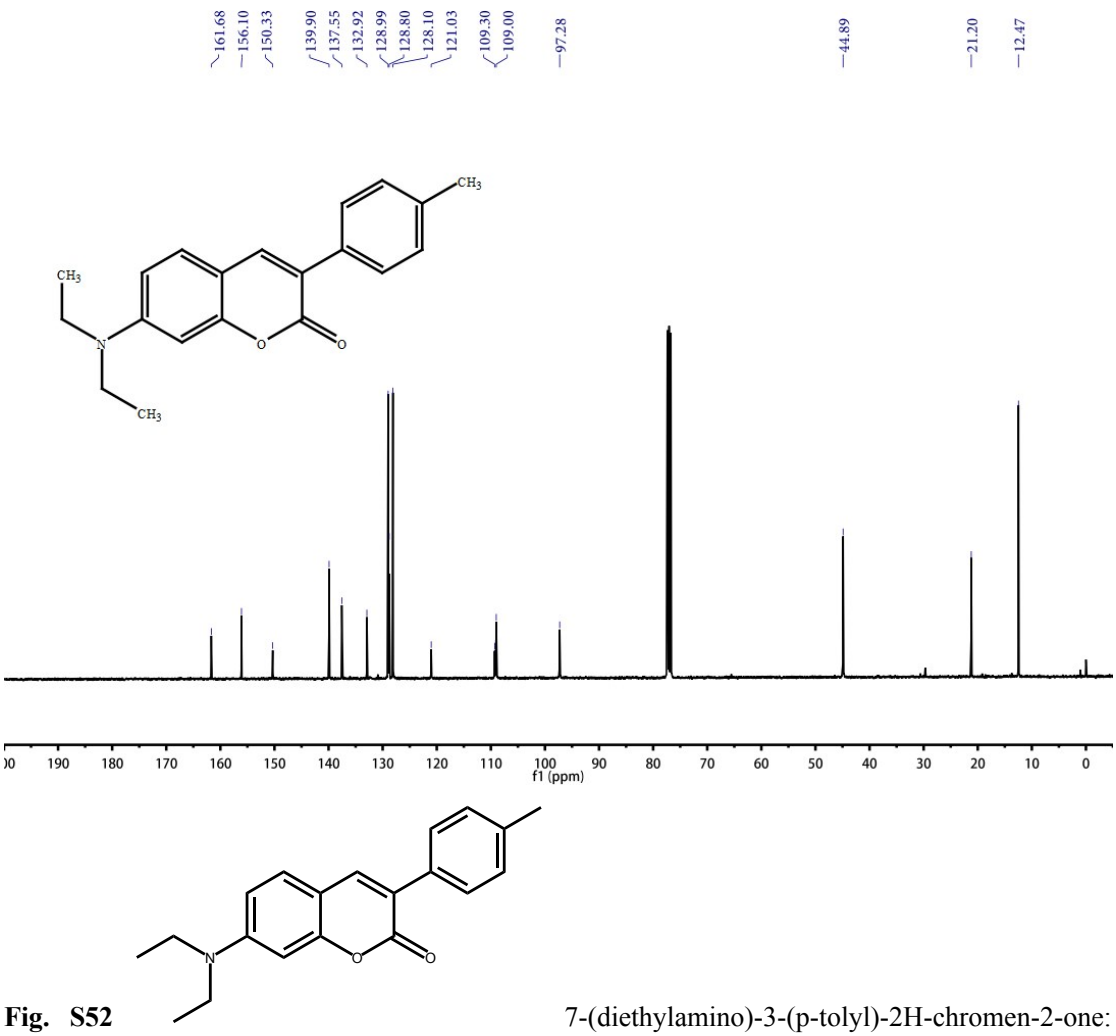

Fig. S52 7-(diethylamino)-3-(p-tolyl)-2H-chromen-2-one: ^{13}C NMR (100 MHz, $CDCl_3$) 161.68, 156.10, 150.33, 139.90, 137.55, 132.92, 128.99, 128.80, 128.10, 121.03, 109.30, 109.00, 97.28, 44.89, 21.20,12.47.

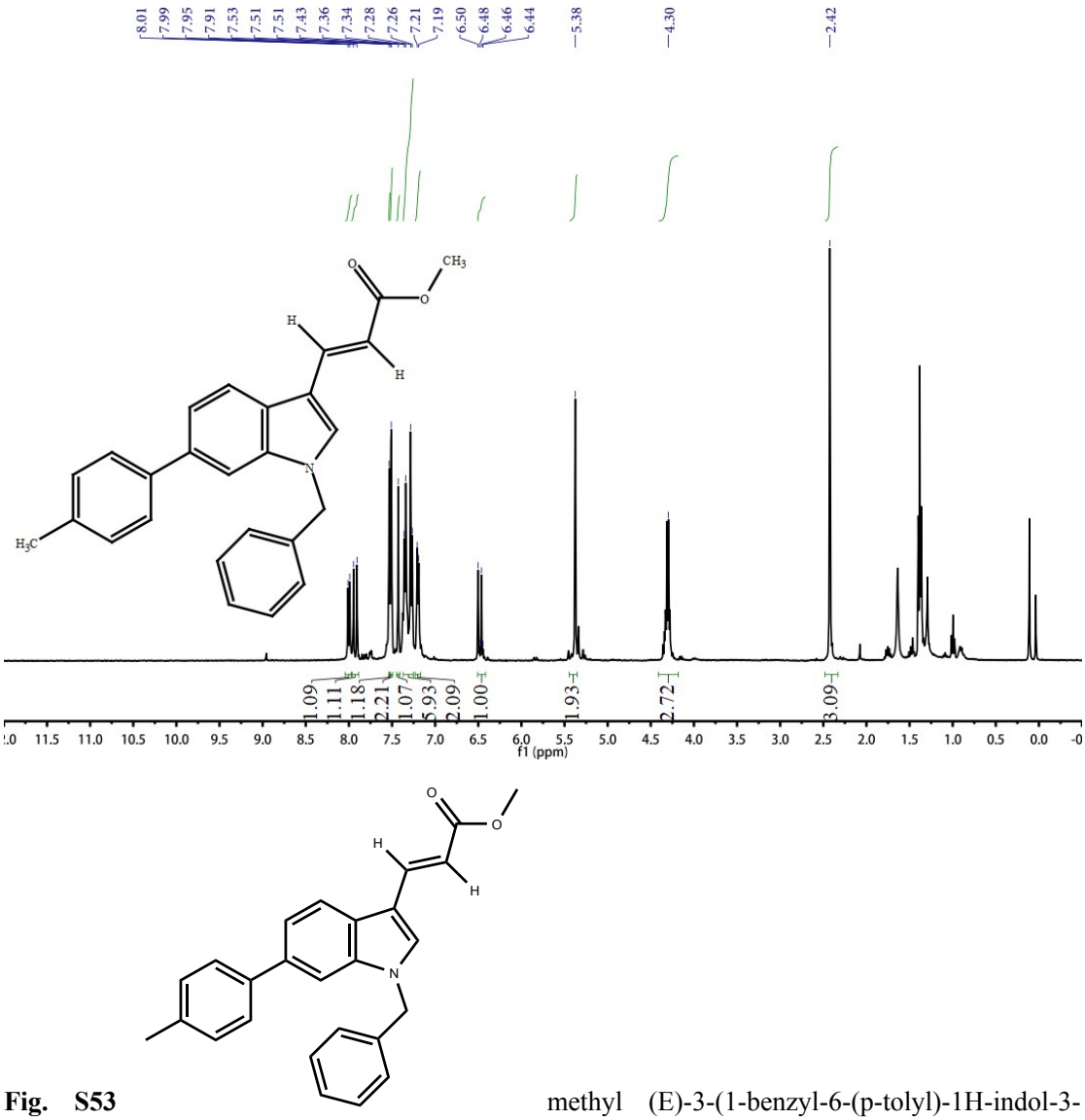

Fig. S53 methyl (E)-3-(1-benzyl-6-(p-tolyl)-1H-indol-3-yl)acrylate: 1H NMR (400 MHz, CDCl3) 8.00 (d, J = 8.2 Hz, 1H), 7.93 (d, J = 16.0 Hz, 1H), 7.53 (s, 1H), 7.52 - 7.49 (d, 2H), 7.43 (s, 1H), 7.37 - 7.25 (m, 6H), 7.20 (d, J = 7.2 Hz, 2H), 6.47 (dd, J = 16.0, 7.0 Hz, 1H), 5.38 (s, 2H), 4.30 (s, 3H), 2.42 (s, 3H).

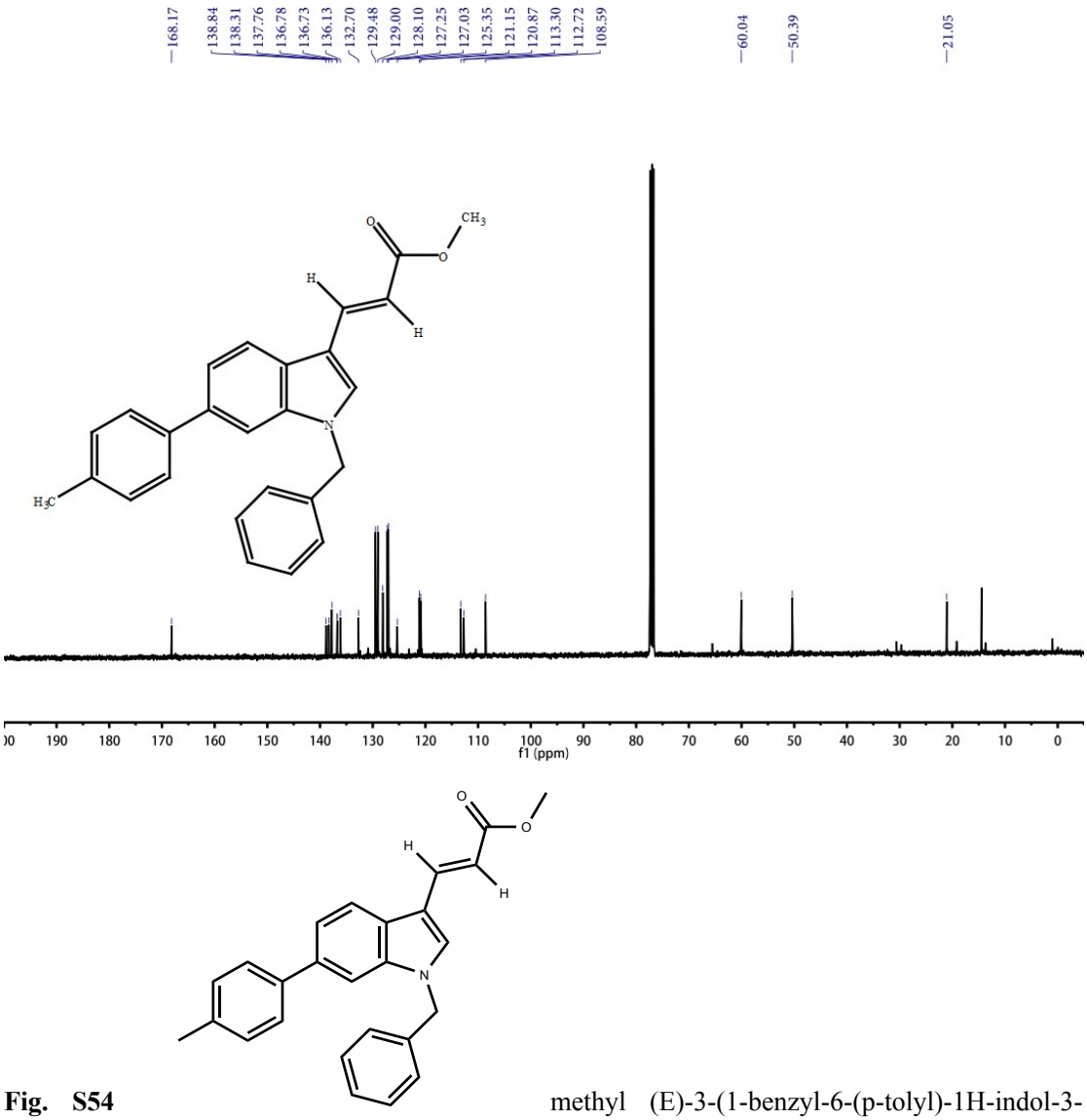

Fig. S54 methyl (E)-3-(1-benzyl-6-(p-tolyl)-1H-indol-3-yl)acrylate:^{13}C NMR (101 MHz, $CDCl_3$) 168.17, 138.84, 138.31, 137.76, 136.78, 136.73, 136.13, 132.70, 129.48, 129.00, 128.10, 127.25, 127.03, 125.35, 121.15, 120.87, 113.30, 112.72, 108.59, 60.04, 50.39, 21.05.